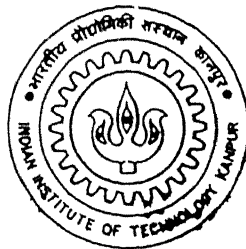


# RESPONSE ANALYSIS OF BURIED CIRCULAR PIPES UNDER 3-DIMENSIONAL SEISMIC LOADING

*A thesis submitted  
in partial fulfilment of the requirements  
for the degree of  
MASTER OF TECHNOLOGY*

*by*  
**Ronanki Siva Sree**



*to the*  
**DEPARTMENT OF CIVIL ENGINEERING  
INDIAN INSTITUTE OF TECHNOLOGY KANPUR**  
June, 1997

SEP 1997

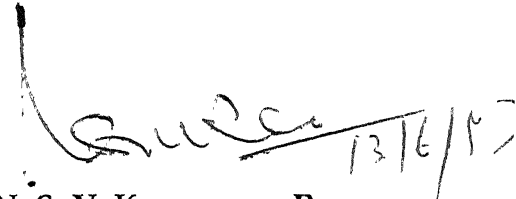
CENTRAL LIBRARY  
KANPUR

Acc. No. A 123751

CE-1997-M-SRE-RES

## Certificate

It is certified that this work entitled **Response analysis of buried circular pipes under three dimensional seismic loading**, by **R. Siva Sree** has been carried out under my supervision and this has not been submitted elsewhere for a degree.



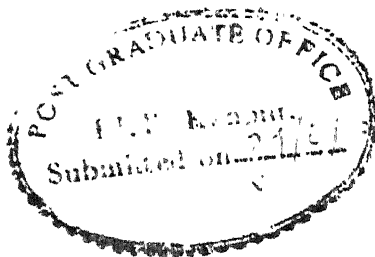
**Dr. N. S. V. Kameswara Rao**

Professor

Department of Civil Engineering

Indian Institute of Technology

Kanpur - 208 016, India



## **Acknowledgements**

I am deeply indebted to Prof. N. S. V. Kameswara Rao for his guidance, encouragement and inspiration. The experience I have gained by working under him is an invaluable possession of my life.

I am also grateful to Prof. M. R. Madhav, Prof. P. K. Basudhar and Prof. Sarvesh Chandra for their invaluable help.

I wish to express heartfelt gratitude towards all of my caring friends, without mentioning their names, who have in all possible ways extended their help as and when needed.

Finally, I would like to thank my parents and sisters for their constant help and encouragement in pursuing my higher studies.

***Ronanki***

# CONTENTS

<b>CONTENTS</b>	<b>i</b>
<b>LIST OF FIGURES</b>	<b>iv</b>
<b>LIST OF TABLES</b>	<b>v</b>
<b>NOTATION</b>	<b>vi</b>
<b>1 INTRODUCTION</b>	<b>1</b>
1.1 General	1
1.2 Literature review	2
1.2.1 Pipes subjected to static loads	2
1.2.2 Pipes subjected to dynamic loads	4
1.2.2.1 Damage analysis	5
1.2.2.1.1 Qualitative analysis	5
1.2.2.1.2 Quantitative analysis	6
1.2.2.2 Quasi-static methods	6
1.2.2.3 Analytical methods	7
1.2.2.4 Numerical methods	8
1.3 Scope of present investigation	10
1.4 Organization of the Thesis	11

<b>2</b>	<b>FORMULATION AND METHOD OF SOLUTION</b>	<b>13</b>
2.1	General	13
2.2	Finite element method	13
2.3	Formulation	15
2.4	Finite element model	18
	2.4.1 Element stiffness matrix	18
	2.4.2 Element mass matrix	23
2.5	Package used and method of solution	23
	2.5.1 About package	23
	2.5.1.1 Structural analysis program(SAP-80)	23
	2.5.2 Equations of motion	24
	2.5.3 Mode superposition method	25
<b>3</b>	<b>RESULTS AND DISCUSSIONS</b>	<b>30</b>
3.1	General	30
3.2	Problem1: Response of buried pipe under static surface loading	30
	3.2.1 Validation of the model	31
	3.2.1.1 Effect of load width-to-radius ratio	32
	3.2.1.2 Effect of radius-to-thickness ratio	32
	3.2.2 Summary	32

3.3	Problem2: Response of buried pipe under seismic loading	39
3.3.1	Validation of the model	39
3.3.1.1	Input data	39
3.3.1.2	Effect of mode shape number	43
3.3.2	Parametric studies	44
3.3.2.1	Effect of three dimensional seismic loading	46
3.3.2.2	Effect of mode shape number	46
3.3.2.3	Effect of $E_p/E_s$ ratio	47
3.3.2.4	Effect of radius-to-thickness ratio	47
3.3.2.5	Effect of embedment depth	47
3.3.2.6	Effect of liquefied soil zone	48
3.3.3	Summary	49
<b>4</b>	<b>CONCLUSIONS ANS SCOPE FOR FUTURE STUDY</b>	<b>52</b>
4.1	General	52
4.2	Conclusions	52
4.3	Scope for future study	52

## REFERENCES

# LIST OF FIGURES

2.1	8 Noded Hexahedron Element in Global and Local Coordinate Systems	19
2.2	Spring, Damping and Mass System	25
3.1	Problem Definition for 3-D Pipe-soil System under Static loading	34
3.2	Finite Element Discretization for 3-D Pipe-soil system under Static loading	35
3.3	Dimensionless Crown deflection vs Load width-to-radius ratio for $H/D = 1$	36
3.4	Dimensionless Crown deflection vs Load width-to-radius ratio for $H/D = 2$	36
3.5	Dimensionless Springline deflection vs Load width-to-radius ratio for $H/D = 1$	37
3.6	Dimensionless Springline deflection vs Load width-to-radius ratio for $H/D = 2$	37
3.7	Dimensionless Crown deflection vs Radius-to-thickness ratio	38
3.8	Problem Definition for 3-D Pipe-soil System under Seismic loading	40
3.9	Finite Element Discretization for 3-D Pipe-soil system under Seismic loading	41
3.10	El Centro (California 1940) earthquake Data	42
3.11	Response spectrum of El Centro earthquake	42
3.12	Crown response vs Mode shape number	43
3.13	Projected Discretized model on x-z plane	45
3.14	Response vs Mode shape number	50
3.15	Response vs $E_p/E_s$ ratio	50
3.16	Response vs Radius-to-thickness ratio	51
3.17	Response vs Embedment depth-to-diameter ratio	51



# LIST OF TABLES

3.1	Response under different earthquakes	43
3.2	Effect of 3-D seismic loading on responses	46
3.3	Effect of liquefied soil zone on responses	48

# Notations

The following notations has been used in this Thesis

$a_x$	Acceleration in x-direction
$a_y$	Acceleration in y-direction
$a_z$	Acceleration in z-direction
$b$	Half width of loading
$B$	Half width of the model
$[B]$	Matrix relating strains to nodal displacements
$[C]$	Damping matrix
$D$	Diameter of pipe
$H$	Depth of embedment
$E_{ls}$	Young's Modulus of liquefied soil
$E_p$	Young's Modulus of pipe
$E_s$	Young's Modulus of soil
$[E]$	Elasticity matrix
$f$	Body force vector
$f^e$	Body force vector of an element
$f_k$	Force component
$J$	Jacobian of transformation
$[J]$	Jacobian matrix
$[K]$	Stiffness matrix
$[K^e]$	Element stiffness matrix
$L$	Differential operator describing the behaviour Lagrangian of the -whole domain
$L$	Length of pipe
$[L]$	Matrix relating strains and displacements
$M_s$	Confined modulus
$[M]$	Mass matrix
$[M^e]$	Element mass matrix

$N_1, N_2, \dots$	Shape functions
$N_i$	Mapping function
$[N]$	Shape function matrix
$nel$	Number of elements
$p$	Intensity of surface loading
$p_i$	Participation factor
$P$	Potential energy
$R$	Radius of pipe
$t$	Thickness pipe
$t$	Time
$t_n$	Time at nth step
$T$	Kinetic energy
$u$	Displacement in x-direction
$u^l$	Relative displacement
$u^e$	Absolute displacement
$u^e$	Approximating function over element
$u_g$	Ground displacement
$u_k$	Displacement component
$\ddot{u}_g$	Ground acceleration
$U$	Mode transformation
$U$	Three dimensional relative displacement
$\dot{U}$	Three dimensional relative velocity
$\ddot{U}$	Three dimensional relative acceleration
$\{U\}$	Nodal displacement vector
$v$	Displacement in y-direction
$w$	Displacement in z-direction
$x_1, x_2, \dots$	Nodal coordinates
$x$	Vector of nodal coordinates
$y_{i,max}$	Maximum response of ith node
$Y$	Vector of normal coordinates
$\delta$	Variation

$\epsilon$	Strain
$\epsilon^e$	Strain over element
$\Gamma$	Surface of domain
$\Gamma^e$	Surface of the element
$\Omega$	Volume of the domain
$\Omega^e$	Volume of the element
$\nu$	Poisson's ratio
$\nu_p$	Poisson's ratio of the pipe material
$\nu_s$	Poisson's ratio of the soil
$\Phi$	Matrix of mode shapes
$\omega$	Frequency
$\rho$	Mass density
$\rho$	Cross-modal coefficient
$\zeta_i$	Damping ratio for mode i

## Abstract

Pipelines as a part of lifeline systems are very much important in normal life and particularly so during and after earthquake. Basic services such as water supply, sewage disposal, gas and petrol supply, electrical and telephone communications etc. may suffer severe damages due to disruption caused to the ground installations including buried pipes. The seismic behaviour of buried pipes is quite different from that of super structures mainly because of inertia forces and ground motion.

The present study is focussed on the response analysis of buried pipes under seismic loading using a 3-D finite element model. Finite element method package, SAP-80 has been used to analyze the pipe-soil system under different load conditions and different soil conditions. Parametric study has been conducted on 1) response of pipe-soil system under static loads and 2) response of pipe-soil system under seismic loads. The parameters considered are - load width-to-radius ratio, radius-to-thickness ratio, embedment depth-to-diameter ratio, mode shape number, modular ratio, 3-D seismic loading and liquified soil zone. The results obtained, have been presented for a wide range of parameters and are compared with those already reported in literature wherever possible.

It has been observed that the present 3-D model can be used effectively to obtain the response of pipe-soil system under different loads.

# Chapter 1

## Introduction

### 1.1 General

Safe and reliable functioning of buried pipelines , as a part of lifeline systems are very much important in normal circumstance and particularly so during and after earthquake. For instance, basic services such as water supply, sewage disposal, gas and petrol supply, electrical and telephone communications etc. may suffer severe damages due to any disruption caused to the under ground installations including buried pipes.

There are three main causes of failures of buried pipelines due to earthquake; 1) excessive axial and bending stresses and deformations in the pipelines created mainly due to the phase difference and change of wave shape between different stations, 2) fault movement during an earthquake, if the pipeline crosses a major fault and 3) inelastic behaviour of soil such as liquefaction. The seismic behaviour of buried pipelines is quite different from that of above-ground structures (super structures) mainly because a) the inertia forces which are the main factors affecting the design of super structures are mainly resisted by the surrounding soil in the case of buried pipelines, b) the ground motion is considered as coherent for most of super structures, while for buried pipelines (being a long continuous system) it is considered as incoherent because of phase difference between different stations and change in shape due to the

variation in soil properties along the pipeline and c) the damage of one super structure is restricted to that structure alone in many cases while the damage at a certain location within the network of pipes will affect the other portions of the system.

## **1.2 Literature review**

The available literature on the buried pipes has been reviewed under the following categories

Pipes subjected to static loads

Pipes subjected to dynamic loads

### **1.2.1 Pipes subjected to static loads**

Most of the analytical and numerical methods available so far represent the soil system as a continuum. Solution techniques for the problem of soil-conduit system can be classified either as analytical methods using classical elasticity theory and shell theory to obtain 'exact' solutions or numerical methods using approximate techniques such as finite difference, finite element and boundary element.

Hoeg (1968) obtained closed form solution of the problem of medium-cylinder interaction analytically by developing static solution for an elastic thin cylinder embedded in a homogeneous, isotropic and elastic medium with surface loading. No-slip condition and full-slip condition at cylinder-medium interface was considered. In the solutions for no-slip case, the radial and tangential

displacements of the cylinder were equated to the corresponding displacements of the cylinder at the medium-cylinder interface. In the solutions for the full-slip case, the radial displacements of the cylinder and medium were equated, but the tangential shear stress was set to zero at the medium-cylinder interface.

Brown (1967) used the finite element method to analyse the forces on rigid culverts under high fills. He used incremental fill sequence technique for the analysis, but the soil medium was assumed to be elastic. Moreover, the interface boundary condition was treated only approximately by using triangular elements which were assigned very high stiffness values compared to fill. Brown et al. (1968) improved the representation of the culvert by using three overlapping triangular elements. Both rigid and flexible culverts were investigated to study the effects of slippage and no slippage.

Anand (1974) studied the stress distribution around shallow buried rigid pipes using finite element method. The study was limited to elastic analysis and depth of embedment equal to one diameter of the pipe. The effect of width of imposed load, modulus ratio etc. on responses are analysed and compared with closed form solutions. Abel et al. (1973) have studied the effect of pipe stiffness, depth of cover and effect of slippage at the interface for an elliptical pipe for surcharge loading. It was found that the effect of Poisson's ratio of pipe material and the soil is negligible and the slip at the interface is beneficial for establishing arching action, particularly for deeply buried pipes.

Prakash et al. (1976) investigated the buried pipe under embankment using finite element method. The parametric studies for height of fill-to-diameter ratio,



diameter-to-thickness ratio and backfill properties were carried out. The effect of sequential construction by assuming linear and non-linear behaviour on responses was studied. Valliappan et al. (1977) analysed the buried pipe under surface pressure by assuming the medium to be elasto-plastic, limited tension material. Conditions of slippage and no-slippage cases are studied by using interface elements. Two different yield criteria, namely, Von-Mises and Drucker's modified Von-Mises, have been adopted for the elasto-plastic idealisation of the medium.

Ramakrishnan (1979) analysed buried pipes in linear and non-linear elastic media by using finite element method. Pipe-soil system was analysed as a soil-structure interaction problem. The pipe-interface-soil was taken as a single unit, where, the pipe is simulated by bar elements, interface by interface elements and soil by 4-CST quadrilateral elements. Non-linear analysis has been carried out simulating stress-strain behaviour by hyperbolic law. The responses like springline thrust, crown pressure, crown deflection, springline deflection, maximum radial pressure and maximum tangential pressure have been studied for various values of parameters, such as radius-to-thickness ratio, modular ratio, semi-load width-to-radius ratio for surface pressures.

### **1.2.2 Pipes subjected to dynamic loads**

In general depending on the method of analysis and the type of surrounding soil the existing literature for dynamic response of buried pipelines, can be classified in the following categories

Damage analysis

Quasi-static methods

Analytical methods

Numerical methods

### **1.2.2 .1 Damage analysis**

#### **1.2.2.1.1 Qualitative damage analysis**

Most of the existing literature concerning buried pipeline damage due to earthquake present a qualitative rather than quantitative description of the damage. Kachadoorian (1976) reviewed damage data from the 1964 Alaska earthquake, the 1968 Mechering earthquake and the 1971 San Fernando earthquake and concluded that the geological environment under the buried pipeline influenced the intensity and frequency of the pipeline damage. Kube (1974), Nasu, Kazama, Morioka and Tamura (1974) have indicated that the pipelines moved closely with the ground in both longitudinal and lateral directions during the seismic wave propagation. Katayama, Kubo and Sato (1975) correlated pipeline damage to pipe size and concluded that smaller pipes are liable to break. Luscher, Black and Nair (1975) discussed briefly the design of the buried portion of Trans-Alaska pipeline. Duke and Moran (1975) and Whitman, Cornell and Tabel-Agha (1975) suggested the use of a reliability/damage level approach to pipeline systems design for various intensities of ground motion.

Ghashi (1977) observed that the damage was maximum in the regions of transition from one type of soil to another. Yeh (1977) determined the range of conservatism of the assumption that the pipe moves with the surrounding soil.

The design formulae for pipe stresses due to oblique incident compressional, shear and Rayleigh surface waves were derived.

#### **1.2.2.1.2 Quantitative damage analysis:**

In addition to the aforementioned studies, some researchers have analysed the quantitative damage of pipelines. Katayma et al.(1975) (1977) and Katayma (1976) analysed the pipeline damage to 1923 Kanto earthquake in terms of damage index (D. I). Kubo (1975) studied the pipeline damage from the 19 71 San Fernando earthquake by dividing the affected regions in to a series of strips. He plotted a graph between the number of breaks per unit length versus maximum acceleration of ground. Katayma et al. (1977) presented a statistical method to analyse seismic damage to 1923 Kanto earthquake employing multivariate regression with observed degree of damage.

#### **1.2.2.2 Quasi-static method of analysis:**

Sakurai and Takahashi (1969), Newmark (1971) and Shah and Chu (1974) analysed the seismic response of underground pipelines to earthquake using the quasi-static method without taking into account soil-pipeline interaction, in which they assumed that the pipeline was flexible enough to follow the deformation of the surrounding soil. Thus by using the maximum values of amplitudes and wavelength of the soil seismic deformation, the maximum pipeline strains are determined. Nelson and Weidlinger (1977, 1978) suggested the use of an 'Interface Response Spectra' while Wang and Cheng (1978) proposed the use of quasi-static approach with soil-pipeline interaction for analysis of buried pipelines subjected to earthquake excitation.

### 1.2.2.3 Analytical methods

Muleski, Ariman and Aumen (1978) and Novak and Hindy (1978) studied the response of buried pipes using shell model. The latter formulated the problem in terms of both deterministic and random vibration. Wang and Fung (1979) proposed a modified Von-Mises failure criterion to evaluate the safety of buried non-homogeneous pipes against earthquakes. Datta et al. (1984) studied the seismic response of large cylindrical shells surrounded by an infinite homogeneous elastic medium. Two different models 1) a beam model 2) Flugge's shell models are used. In their work, full dynamic interaction between the shell and the surrounding soil was taken into account.

Datta and Mashaly (1986) obtained the response of buried pipelines to random earthquake forces using lumped mass model. The earthquake was considered as a stationary random process characterized by a power spectral density function (PSDF). The cross spectral density function between two random inputs along the pipe length was defined in terms of local earthquake PSDF. The soil resistance to dynamic excitation along the pipe length has been obtained in frequency independent impedance functions which were derived from half-space analysis and Mindlin's static stresses with in the soil due to point loads. In their study they considered the cross terms in the soil stiffness and damping matrices. Parametric studies have been done for the influence of cross terms in the soil stiffness and damping on the response of the pipe.

Zerva et. al. (1988) developed a model for near source ground motions, in which the excitation was modelled as a random process based on the earthquake magnitude and the site characteristics. Power and cross spectral densities of acceleration at any station on the ground surface, cross correlation coefficients and spectral densities of differential accelerations are the out puts from the model. The results of the application of model to the earthquake of January 29, 1981 in Lotung, Taiwan, has been compared with actual earthquake data records at the Strong Motion Array in Taiwan (SMART). The motions obtained by the above analytical model are used as input motions for the study of the dynamic response of the pipelines. The response of the two different pipeline structural models, 1) pipelines with soft joints and 2) continuous pipelines to perfectly and partially correlated random input motions in the axial, lateral and vertical directions are investigated and the significance of the spatial variation of ground motion was also examined.

Datta and Mashaly (1990) proposed a method based on spatial discretization of the pipe with nodal lumped masses for the transverse response of suspended spans of submarine pipelines to random excitation. The response was obtained in frequency domain using spectral analysis. They have taken into account the pressure drag effect and spatial correlation of seismic excitations along the pipe length in their parametric studies.

#### **1.2.2.4 Numerical methods:**

Numerical methods such as Finite difference method, Finite element method, Boundary element method and Hybrid methods were employed by several

investigators to obtain solutions to dynamic soil-pipe interaction problems. Ang and Newmark (1963) computed response of the underground structures using finite difference method. Farhoomand and Wilson (1970) proposed the non-linear finite element method for analysing the blast response of the underground structures. Haldor et al. (1980) evaluated the seismic response of submarine concrete coated steel pipes buried in a porous bed, using a plane strain finite element model. The non linear soil behaviour was treated by an equivalent linear method and the effect of energy dissipation in the porous soil medium was taken into account by standard viscous boundaries developed by Lysmer and Kuhlemeyen (1969).

Datta et.al.(1984) obtained the displacements and stresses in buried pipeline under dynamic loading. A hybrid technique, combining a finite element method with the eigen function expressions was used for the dynamic response of pipe. The line was modelled as a circular cylindrical shell of small thickness, and the incidence disturbances are assumed as plane waves, moving perpendicular to the axis of pipeline. Two problems 1) the pipe surrounded by a homogeneous soft soil 2) the pipe lying in a cylinder of soft soil which is surrounded by a hard material have been studied.

Yaw-Huei Yeh et.al. (1985) proposed a simplified pipe model with beam on time dependent elastic foundation for the dynamic response of buried pipelines in soil liquefaction environment. A finite difference method involving both temporal and spatial variables was used for the response during earthquakes. The influence of a) soil stiffness, b) loading speed of pipe end, c) initial crookedness and d)

supporting length of the pipe segment inside the liquefied region on the pipe response are studied.

Shakib and Abdolsalami (1995) investigated the response of the buried pipeline to seismic excitation in lateral and longitudinal directions in time domain. The pipeline was idealized with assemblage of 2 D beam element, and a discrete lumped mass model was employed to the pipe motions. The soil stiffness and damping matrices are derived from static and dynamic continuum solutions. The main features of this method are that it can take into account any boundary conditions that needs to be imposed at the pipeline ends and also, it can consider the cross terms in the soil stiffness and damping matrices. Numerical studies are conducted to investigate the effect of pipeline length, element length, end conditions of pipe, embedment depth and cross terms of soil stiffness and damping matrices in homogeneous medium on the response.

Stamos and Beskos (1995) have proposed a numerical method (boundary element method) for determining the dynamic response of three dimensional large underground elastic structures. For transient dynamic disturbance numerical inversion of Laplace transform was used for computing response in time domain, whereas for harmonic disturbances the response was obtained directly in the frequency domain.

### **1.3 Scope of present investigation**

Based on the brief survey carried out, it can be pointed out that an accurate and feasible model for seismic response of buried pipeline is not available. The 2 D

domain discretization models provide approximate solutions with different levels of accuracy. Some of 2 D models with absorbing boundaries provide an improvement over the other methods but are not associated with the three dimensional earthquake loading. Little research has been done on seismic analysis of pipes under general earthquake loading and liquefaction conditions.

To achieve above objectives, response of buried circular pipes subjected to three dimensional seismic loading has been studied using three dimensional finite element method in the present investigation. Finite element method based package structural analysis programs (SAP-80) has been used in the present study. Three dimensional solid elements are used for both discretizing the pipe and the surrounding soil. Large three dimensional model, reflect small amount of energy through the boundaries has been considered. Modal superposition method has been used to evaluate the response of pipe under three dimensional earthquake loading.

## **1.4 Organization of the Thesis**

The work that has been carried out in this thesis is presented in the following manner.

Chapter 2 describes the general principles and basic concepts of finite element method. 3 D discretization and application of finite element method to dynamic analysis of pipe-soil system are described. The details of package SAP-80, and mode superposition method have been presented briefly.



In chapter 3, the results and discussions are presented. Two problems 1) response of buried pipe under static loading and 2) response of buried pipe under seismic loading have been analysed. The effect of parameters like load width-to-radius ratio, radius-to-thickness ratio, depth of embedment-to-diameter ratio on responses like horizontal springline displacement, vertical crown displacement are studied in case of static analysis. In seismic study, the effect of parameters like load width-to-radius ratio, radius-to-thickness ratio, depth of embedment-to-diameter ratio, mode shape number, 3 D seismic loading and liquefaction zone on responses like horizontal springline displacement, vertical crown displacement are studied.

Conclusions are summarized in Chapter 4. Possible extensions of the present work are indicated.

## **Chapter 2**

### **Formulation and Method of solution**

#### **2.1 General**

The seismic soil-pipe interaction deals with the response of pipe under seismic loading. Since soil exists as semi-infinite half space, numerical methods have to incorporate the notion of infinity in the formulation. Numerical methods like Integral equation method, boundary element method can handle infinite domains naturally, where as domain discretization methods like finite difference, finite element methods can not be applied to semi-infinite domains directly. A way-out of handling such infinite domains is to consider a finite (computational) domain for discretization with an approximate boundary conditions (energy absorbing) on the finite domain, or a large domain with a boundary which reflects little energy.

#### **2.2 Finite element method:**

Many engineering problems encountered in the present practice deal with systems with distributed parameters. The application of mechanics to such a systems often lead to a system of partial differential equations. In case the domain and the equations are simple, the solution can be obtained in exact form,

using Fourier, Laplace transform methods etc. Exact solutions to general partial differential equations are difficult to obtain due to irregular and geometrically complicated domains. Consequently, various methods of finding suitable solutions have been under continuous development. Finite difference method and variational methods are more popular ones. The difficulty in applying these methods lies in constructing approximating functions of the dependent variable, which need to satisfy the geometric boundary conditions on irregular domains. The finite element method which is an offshoot of the classical methods overcomes these difficulties and gained wide popularity and acceptance.

In finite element method (FEM) the given domain is subdivided into a finite number of small sub domains. The subdomains, called finite elements, are of geometrically simple shapes, and permit a systematic construction of the approximating functions. Generally these approximating functions are algebraic polynomials developed using interpolation theory, and are called interpolation functions. Since the approximating functions are defined element-wise, the accuracy of the approximation can be improved by increasing the number of elements. Generally the interpolation points, called nodes are placed on the boundary of the element such that they uniquely define the element geometry. Additional nodes which may be required to define the interpolation functions can be placed either inside or on the boundary of the element. The boundary nodes also facilitate in connecting the adjacent elements together by ensuring the

primary degree of freedom to be the same at the common nodes. The nodal values of the element displacement uniquely defines the function values within the element and they form the basic unknowns of the problem.

## 2.3 Formulation

In this section the basic formulation of finite element method is discussed. A displacement type formulation uses nodal displacements  $u$ ,  $v$ ,  $w$  as primary variables. Variational formulation has been utilized to develop the procedure for spatial discretization. Hamilton's principle has been used to construct the functional. The principle is stated as follows (Desai and Abel 1972),

Among all possible time histories of displacement configurations which satisfy compatibility conditions and which also satisfy conditions at time  $t_1$  and  $t_2$ , the history which is the actual solution makes the Lagrangian functional minimum.

This can be stated as

$$\delta \int_{t_1}^{t_2} L dt = 0 \quad (2.1)$$

where  $\delta$  indicates the variation of the integral and  $L$  is the Lagrangian which can be expressed as

$$L = T - P - W \quad (2.2)$$

where  $T$ ,  $P$  and  $W$  are kinetic energy, strain energy and potential energy of the applied loads. Accordingly

$$L = \frac{1}{2} \int_{\Omega} [\dot{u}^T \rho \dot{u} - \epsilon^T \sigma] dv + \int_{\Omega} u^T f dv + \int_{\Gamma} u^T \tau ds \quad (2.3)$$

where  $\rho$  denotes the mass density of the material; dots denote the time derivative of the variables.

Lagrangian  $L$  of the whole domain can be assembled as sum of the contributions over each of the elements, i.e.

$$L = \sum_{i=1}^{nel} \left[ \frac{1}{2} \int_{\Omega^e} \{ \dot{u}^{eT} \rho \dot{u}^e - \epsilon^{eT} \sigma^e \} dv + \int_{\Omega^e} \{ u^{eT} f^e \} dv + \int_{\Gamma^e} \{ u^{eT} \tau^e \} ds \right] \quad (2.4)$$

Substituting for the approximate displacement vector  $u^e$  defined over each of the element and stress strain relations in the above equation (Eq. 2.4) results in the following expression

$$L = \sum_{i=1}^{nel} \left[ \frac{1}{2} \int_{\Omega^e} \left( \rho \{ \dot{u}^e \}^T [N]^T [N] \{ \dot{u}^e \} - \{ u^e \}^T [B]^T [E] [B] \{ u^e \} \right) dv + \int_{\Omega^e} \{ u^e \}^T [N]^T \{ f^e \} dv + \int_{\Gamma^e} \{ u^e \}^T [N]^T \{ \tau^e \} ds \right] \quad (2.5)$$

Hereafter the summation symbol is omitted for the sake of conciseness and wherever elemental quantities appear, usual summation (assembly) over the elements is implied. Substituting the above expressions for Lagrangian in Eq. 2.1 gives the expression

$$\begin{aligned}
& \int_{t_1}^{t_2} \left[ \rho \{ \delta \dot{u}^e \}^T \left( \int_{\Omega} [N]^T [N] \{ \dot{u}^e \} d\nu \right) - \{ \delta \dot{u}^e \}^T \left( \int_{\Omega} [B]^T [E] [B] \{ u^e \} d\nu \right. \right. \\
& \quad \left. \left. - \int_{\Omega} [N]^T \{ f^e \} d\nu - \int_{\Gamma} [N]^T \{ \tau^e \} ds \right) \right] dt = 0
\end{aligned} \tag{2.6}$$

Integrating the first term results in the Eq. 2.7,

$$\begin{aligned}
& \int_{t_1}^{t_2} \left[ \rho \{ \delta \dot{u}^e \}^T \int_{\Omega} [N]^T [N] \{ \dot{u}^e \} d\nu \right] dt = \left[ \rho \{ \delta u^e \} \int_{\Omega} [N]^T [N] \{ \dot{u}^e \} d\nu \right]_{t_1}^{t_2} \\
& \quad - \int_{t_1}^{t_2} \left[ \rho \{ \delta u^e \} \int_{\Omega} [N]^T [N] \{ \ddot{u}^e \} d\nu \right] dt
\end{aligned} \tag{2.7}$$

Substituting this expression in the Eq. 2.6 results in the following expression

$$\begin{aligned}
& \left[ \{ \delta u^e \} \int_{\Omega} \rho [N]^T [N] \{ \dot{u}^e \} d\nu \right]_{t_1}^{t_2} \\
& - \int_{t_1}^{t_2} \left( \delta u^e \right) \left[ \int_{\Omega^e} \left( \rho [N]^T [N] \{ \ddot{u}^e \} + [B]^T [E] [B] \{ u^e \} \right) d\nu \right. \\
& \quad \left. - \int_{\Omega} [N]^T \{ f^e \} d\nu - \int_{\Gamma} [N]^T \{ \tau^e \} ds \right] dt = 0
\end{aligned} \tag{2.8}$$

The first term in the right hand side vanishes because the displacement configurations should satisfy the boundary conditions at times  $t_1$  and  $t_2$  (Hamilton's principle) i.e. the variation  $\{ \delta u^e \}$  should be equal to zero at times  $t_1$

and  $t_2$  rest of the expression inside the parenthesis should vanish because the variation is arbitrary. The resulting equation can be written as

$$[M^e]\{\ddot{u}^e\} + [K^e]\{u^e\} = \{P^e\} \quad (2.9)$$

where  $[M^e]$  is element mass matrix and is given by

$$[M^e] = \int_{\Omega^e} \rho [N]^T [N] dv \quad (2.10)$$

Assembling the element matrices results in a system of differential equations (equations of motion) governing the behaviour the body as follows

$$[M]\{\ddot{U}\} + [K]\{U\} = \{P\} \quad (2.11)$$

Here the vectors  $U$ , and  $P$  are time dependent.

## 2.4 Finite element model

An eight noded brick (solid) element is considered as the basic element. Both the pipe and the surrounding soil has been discretized with the same eight noded elastic elements. The governing equation the motion in which matrices  $[M]$  and  $[K]$  are assembled from the individual element matrices. The element mass and stiffness matrices are obtained as described in the following section.

### 2.4.1 Element stiffness matrix

An eight noded isoparametric element is shown in global and local coordinate system in Figure 3.1. Since the local coordinates range from -1 to +1, the

element is a cube with a side of 2 units long and origin of the system at its centroid. The actual element could be any shape with six-faces. The coordinate mapping which relates the two coordinate systems can be expressed as (Equation 2.13)

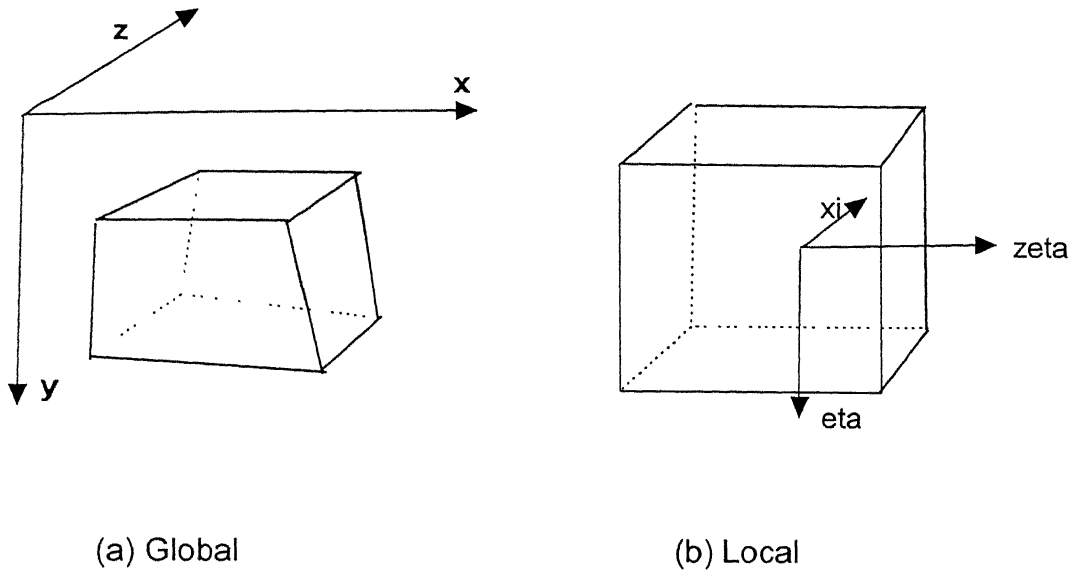


Figure 2.1: 8 noded Hexahedron Element  
in Global and Local Coordinate Systems

$$x = [N_i] \{x_i\} \quad (2.12)$$

where  $x$  and  $x_i$  are the vectors of independent variables in global and local coordinate system respectively, and coordinates for node  $i$  respectively;  $[N_i]$  is a diagonal sub matrix of order equal to the number of space dimensions (3). Each



of its entry equals to mapping function of the node. The subscript  $i$  varies from 1 to 8.

$$X = [x \ y \ z]^T \quad (2.13)$$

$$[N_i] = \begin{bmatrix} N_i & 0 & 0 \\ 0 & N_i & 0 \\ 0 & 0 & N_i \end{bmatrix} \quad (2.14)$$

$$X_i = [x_i \ y_i \ z_i]^T \quad (2.15)$$

The mapping function can be expressed as follows (Desai and Abel 1972)

$$N_i = (1 + \zeta_i \zeta)(1 + \eta_i \eta)(1 + \xi_i \xi) \quad (2.16)$$

where  $\zeta_i$ ,  $\eta_i$ , and  $\xi_i$  are coordinates of the node  $i$  and take either +1 or -1.

The displacement vector  $u$  can be expressed in terms of its nodal values using the shape function expressed in the local coordinate system of the element. Since isoparametric formulation is being adopted the shape functions are same as the coordinate mapping function of the element. Hence,

$$u = [N_i] \{u_i\} \quad (2.17)$$

Using elastic constitutive relations, stresses can be expressed as

$$\sigma = [E] \epsilon \quad \text{and} \quad \sigma^e = [E] \epsilon^e \quad (2.18)$$

where  $[E]$  denotes the elasticity matrix and for three dimensional solid element it can be expressed as,

$$[E] = \frac{E}{(1+\nu)(1-2\nu)} \begin{bmatrix} 1-\nu & \nu & \nu & 0 & 0 & 0 \\ \nu & 1-\nu & \nu & 0 & 0 & 0 \\ \nu & \nu & 1-\nu & 0 & 0 & 0 \\ 0 & 0 & 0 & \frac{1-\nu}{2} & 0 & 0 \\ 0 & 0 & 0 & 0 & \frac{1-\nu}{2} & 0 \\ 0 & 0 & 0 & 0 & 0 & \frac{1-\nu}{2} \end{bmatrix} \quad (2.19)$$

Assuming small strain theory, strains can be defined in terms of displacements using differential operator  $[L]$  as

$$\epsilon = [L]u \quad (2.20)$$

for three dimensional problems the differential operator  $[L]$  is given by,

$$[L] = \begin{bmatrix} \frac{\partial}{\partial x} & 0 & 0 \\ 0 & \frac{\partial}{\partial y} & 0 \\ 0 & 0 & \frac{\partial}{\partial z} \\ \frac{\partial}{\partial y} & \frac{\partial}{\partial x} & 0 \\ 0 & \frac{\partial}{\partial z} & \frac{\partial}{\partial y} \\ \frac{\partial}{\partial z} & 0 & \frac{\partial}{\partial x} \end{bmatrix} \quad (2.21)$$

Similar relations hold for elemental quantities also, element strains can be expressed as

$$\epsilon^e = [L]u^e = [L][N]\{u^e\} = [B]\{u^e\} \quad (2.22)$$

where matrix [B] relates element strains to nodal displacement variables, given by

$$[B] = [L][N] \quad (2.23)$$

The differential operator [L] contains derivatives with respect to physical coordinates. The derivatives have to be computed using Jacobian transformation from local coordinate space to global coordinate space. The Jacobian can be expressed as

$$[J] = \begin{bmatrix} \sum N_{i,\zeta} x_i & \sum N_{i,\zeta} y_i & \sum N_{i,\zeta} z_i \\ \sum N_{i,\eta} x_i & \sum N_{i,\eta} y_i & \sum N_{i,\eta} z_i \\ \sum N_{i,\xi} x_i & \sum N_{i,\xi} y_i & \sum N_{i,\xi} z_i \end{bmatrix} \quad (2.24)$$

The ‘,’ indicates differentiation with respect to the variable following symbol and the symbol  $\sum$  indicates summation over the number of nodes of the element (8 here), viz.

$$\begin{aligned} \sum N_{i,\zeta} x_i &= \frac{dN_1}{d\zeta} x_1 + \frac{dN_2}{d\zeta} x_2 + \frac{dN_3}{d\zeta} x_3 + \frac{dN_4}{d\zeta} x_4 \\ &\quad + \frac{dN_5}{d\zeta} x_5 + \frac{dN_6}{d\zeta} x_6 + \frac{dN_7}{d\zeta} x_7 + \frac{dN_8}{d\zeta} x_8 \end{aligned} \quad (2.25)$$

The stiffness matrix of the element now can be expressed as

$$[K^e] = \int_{-1}^{+1} \int_{-1}^{+1} \int_{-1}^{+1} [B]^T [E][B] ||J|| d\zeta d\eta d\xi \quad (2.26)$$

where  $||J||$  denotes the determinant of Jacobian.

## 2.4.2 Element mass matrix

The element mass matrix can be expressed as (Desai and Abel 1972)

$$[M^e] = \int_{-1}^{+1} \int_{-1}^{+1} \int_{-1}^{+1} \rho [N]^T [N] ||J|| d\zeta d\eta d\xi \quad (2.27)$$

The mass matrix defined by the above Eq. 2.27 is called consistent mass matrix because the same shape functions  $[N]$  are used to generate the stiffness matrix. Often a diagonal form of the mass matrix is adopted assuming the mass of the body is concentrated only at the nodes of the body. This form of the matrix is diagonal and is called lumped mass matrix.

## 2.5 Package used and method of solution

In this section a brief description of the package used in this study and the method of solution has been presented.

### 2.5.1 About package

#### 2.5.1.1 Structural Analysis Program (SAP-80, 1984)

It is a general purpose finite element structural analysis program for the linear static and dynamic analysis. Its development started as early as 1964 and it was

probably one of the very first codes based on finite elements. This is the result of over ten years of research and development by E. L. Wilson\* at the university of California, Berkeley. This program has the capability to analyze very large three dimensional systems. With SAP-80 analytical capabilities in terms of elasticity, temperature and dynamic analysis are classified into different options. The elements available in SAP-80 can be mixed with others within the same option analysis. Material properties can be (for two dimensional) isotropic, orthotropic, temperature dependent, and anisotropic. Boundary conditions can only be defined with respect to global Cartesian axes. The input results can be checked by plotting. Output results can also be plotted. (SAP-80 manual, 1984).

### 2.5.2 Equations of motion

In earthquake-prone regions, the principal problem of dynamics is the behaviour of structure subjected to earthquake-induced motion of the ground. If the displacement of the ground is denoted by  $u_g$ , the total (or absolute) displacement of the mass by  $u'$ , and the relative displacement between mass and ground by  $u$  (Fig. 3.2), then at each instant of time these displacements are related by

$$u'(t) = u(t) + u_g(t) \quad (2.28)$$

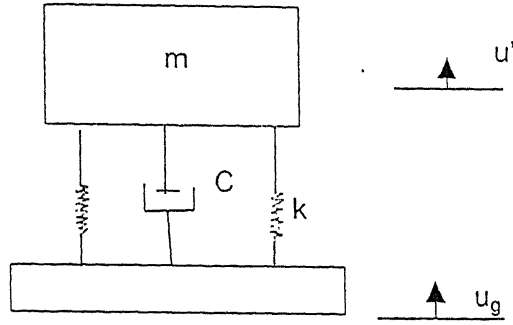


Figure 2.2 Spring, Damping and Mass System

Considering the equilibrium of system shown in Fig 3.2

$$m\ddot{u}' = -k(u' - u_g) \quad (2.29)$$

Using the Equations 2.28 and 2.29 and assembling element mass, damping and stiffness matrices, the equations of the motion of the system can be obtained as

$$M\ddot{U}(t) + C\dot{U}(t) + KU(t) = M\ddot{u}_g(t) \quad (2.30)$$

where  $M$ ,  $C$  and  $K$  are mass, damping and stiffness matrices, respectively. The three dimensional relative displacement, velocity and accelerations are indicated by  $U$ ,  $\dot{U}$  and  $\ddot{U}$ .

### 2.5.3 Mode superposition method (Wilson et al. 1981)

To solve the equation (2.30) mode superposition method has been used in the present study. The mode superposition solution involves the introduction of the transformation

$$U = \Phi Y \quad (2.31)$$

where  $\Phi$  is the matrix containing three dimensional mode shapes of the system and  $Y$  is the vector of normal co-ordinates. The introduction of this transform and the premultiplication of Equation 2.30 by  $\Phi^T$  yields

$$\Phi^T M \Phi \ddot{Y} + \Phi^T C \Phi \dot{Y} + \Phi^T K \Phi Y = \Phi^T M \ddot{u}_g \quad (2.32)$$

For proportional damping the mode shapes have the following properties:

$$\phi_i^T M \phi_i = m_i \quad (2.33)$$

$$\phi_i^T K \phi_i = \omega_i^2 m_i \quad (2.34)$$

$$\phi_i^T C \phi_i = 2\zeta_i \omega_i m_i \quad (2.35)$$

in which  $\phi_i$  is the  $i$ th column of  $\Phi$  representing the  $i$ th mode shape,  $m_i$  is the  $i$ th modal mass, and  $\zeta_i$  is the damping ratio for mode  $i$ . Due to the orthogonality properties of the mode shapes, all modal coupling terms of the form  $\phi_i^T A \phi_j$  are zero for  $i \neq j$ . Thus, Equation 2.32 reduces to a set of uncoupled equations in which the typical 'modal' equation is of the following form

$$\ddot{Y}_i + 2\zeta_i \omega_i \dot{Y}_i + \omega_i^2 Y_i = p_i \ddot{u}_g \quad (2.36)$$

where

$$p_i = \frac{\phi_i^T M}{m_i} \quad (2.37)$$

is the participation factor for mode  $i$ .

The following equation can be solved for the response  $y_i(t)$

$$\ddot{Y}_i + 2\zeta_i \omega_i \dot{Y}_i + \omega_i^2 Y_i = \ddot{u}_g(t) \quad (2.38)$$

At the point in time where  $|y_i(t)|$  is maximum, the response is defined as  $y_{i,\max}$ . A plot of this maximum displacement versus the frequency  $\omega_i$  for each  $\zeta_i$  is by definition the displacement response spectrum (Wilson et al. 1981) for the earthquake  $\ddot{u}_g(t)$ .

If the dynamic loading on the structure is specified in terms of displacement spectrum, then the maximum response of each mode is given by

$$Y_{i,\max} = p_i y_{i,\max} \quad (2.39)$$

Therefore, the maximum contribution of mode  $i$  to the total response of the structure is

$$U_{i,\max} = \phi_i p_i y_{i,\max} \quad (2.40)$$

For all modes  $y_{i,\max}$  is, by definition, positive. The maximum modal displacement  $U_{i,\max}$  is proportional to the mode shape  $\phi_i$ , and the sign of the proportionality constant is given by the sign of the modal participation factor. Therefore, each maximum modal displacement has a unique sign. Also, the maximum internal modal forces, which are consistently evaluated from the maximum modal displacements, have unique sign.

In 3D seismic analysis, for combining modal maxima the square-root-of-sum-of-squares method causes significant errors (Wilson et al. 1981). A complete quadratic combination (CQC) method which reduces errors is used for combining the modal responses (Wilson et al. 1981). The CQC method requires that all modal response terms be combined by the application of the following equations:



For a typical displacement component,  $u_k$ :

$$u_k = \sqrt{\sum_i \sum_j (u_{ki} \rho_{ij} u_{kj})} \quad (2.41)$$

and for a typical force component,  $f_k$ :

$$f_k = \sqrt{\sum_i \sum_j (f_{ki} \rho_{ij} f_{kj})} \quad (2.42)$$

where  $u_{ki}$  is a typical component of the modal displacement response vector,  $U_{i,\max}$ , and  $f_{ki}$  is a typical force component which is produced by the modal displacement vector,  $U_{i,\max}$ .

This combination formula is of complete quadratic form which includes all cross-modal terms, and these cross-modal terms may have positive or negative values depending on whether the corresponding modal response have the same or opposite signs. The signs of modal response are, therefore, an important key to the accuracy of the CQC method.

In general the cross-modal coefficients,  $\rho_{ij}$ , are functions of the duration and frequency content of the loading and of the modal frequencies and damping ratios of the structure. For a constant modal damping, the expression for cross-modal coefficient is

$$\rho_{ij} = \frac{8\zeta^2(1+r)r^{3/2}}{(1-r^2)^2 + 4\zeta^2 r(1+r)^2} \quad (2.43)$$

where  $r = \omega_j / \omega_i$  and  $\zeta$  is modal damping.

Using the above method of solution and SAP-80 package, response of buried pipe under different loads are studied. The results obtained are presented in Chapter 3.

## Chapter 3

### Results and Discussions

#### 3.1 General

The formulation described in the previous chapter is applied to solve 1) the response of buried pipe under static loading and 2) the response of buried pipe under earthquake loading. The basic assumptions are as follows

- 1) the soil is an infinite, elastic, homogeneous and isotropic medium.
- 2) the pipe is circular in shape , long without joints and elastic.
- 3) the pipe is straight and horizontal i.e. there is no level difference between the two ends of the pipe.
- 4) a perfect bond between pipe and soil i.e. during vibration the displacement of pipe must be equal that of adjacent soil.

#### 3.2 Problem 1: Response of buried pipe under static surface loading.

The response of buried pipe-soil system subjected to static surface loading is analysed with the present 3D model. Problem definition and a part of the discretized domain are shown in Figures 3.1 and 3.2.  $L$  and  $D$  are length, and diameter of pipe respectively;  $B$  and  $b$  are half width of the model and half width of loading; and  $H$  and  $t$  are the depth of embedment and thickness of pipe

respectively. The geometry and material properties of the problem analyzed are as follows

Size of the model :  $7.3 \times 10 \times 4.8$  m

Number of elements: 256

Young's Modulus of the soil medium  $E_s = 1 \times 10^4$  kPa

Poisson's ratio of the soil medium  $\nu_s = 0.3$

Young's Modulus of the pipe  $E_p = 4.0 \times 10^6$  kPa

Poisson's ratio of the pipe  $\nu_p = 0.2$

Length of the pipe  $L = 10$  m

Diameter of the pipe  $D = 0.96$  m

Depth of embedment  $H = 0.96$  or  $1.92$  m

The results obtained are non-dimensionalised as follows,

the crown (Fig. 3.1) deflections and springline (Fig. 3.1) deflections are non dimensionalised by  $pxR / M_s$  where  $p$  is the intensity of the surface loading,  $M_s$  is confined modulus equal to  $E_s(1 - \nu_s) / (1 + \nu_s)(1 - 2\nu_s)$ , and  $R$  is the radius of the pipe.

### 3.2.1 Validation of the model

The effect of some parameters on the responses like crown displacement and springline displacement are studied and compared with the available results reported By Ramakrishnan (1979) for validation of the present model. The effect of following parameters on responses are studied

- a) variation of responses with load width to radius ratio ( $b/R$ )
- b) variation of responses with radius to thickness ratio ( $R/t$ )

### 3.2.1.1 Effect of load width-to-radius ratio

The responses of pipe for various  $b/R$  ratios have been studied. They are studied for a  $R/t$  ratio of 20 and  $E_p/E_s$  of 400.  $H/D$  ratios 1 and 2 have been considered.

**Crown deflection:** The dimensionless crown deflection variation with  $b/R$  is shown in Fig. 3.3 and Fig. 3.4 . Crown deflection increases with  $b/R$  ratio up to a value 4, beyond that the deflections tends to be constant.

**Springline deflection:** The dimensionless springline deflection variation with  $b/R$  is shown in Fig. 3.5 and Fig. 3.6 . Springline deflection increases with  $b/R$  ratio up to a value 4, beyond that the deflections tends to be decreased.

### 3.2.1.2 Effect of radius-to-thickness ratio

The responses have been studied for various  $R/t$  ratios for  $b/R = 1$ . The range of  $R/t$  used are 15 to 40. Modular ratio taken for this study is 400.

**Crown deflection:** The maximum diametrical deflection occurs at the pipe crown relative to invert. The variation of dimensionless crown deflections with  $R/t$  ratio has been plotted in Fig. 3.7. The crown deflection increases with increasing  $R/t$  ratio, but the large increase in the thickness changes the crown deflection only by a small amount.

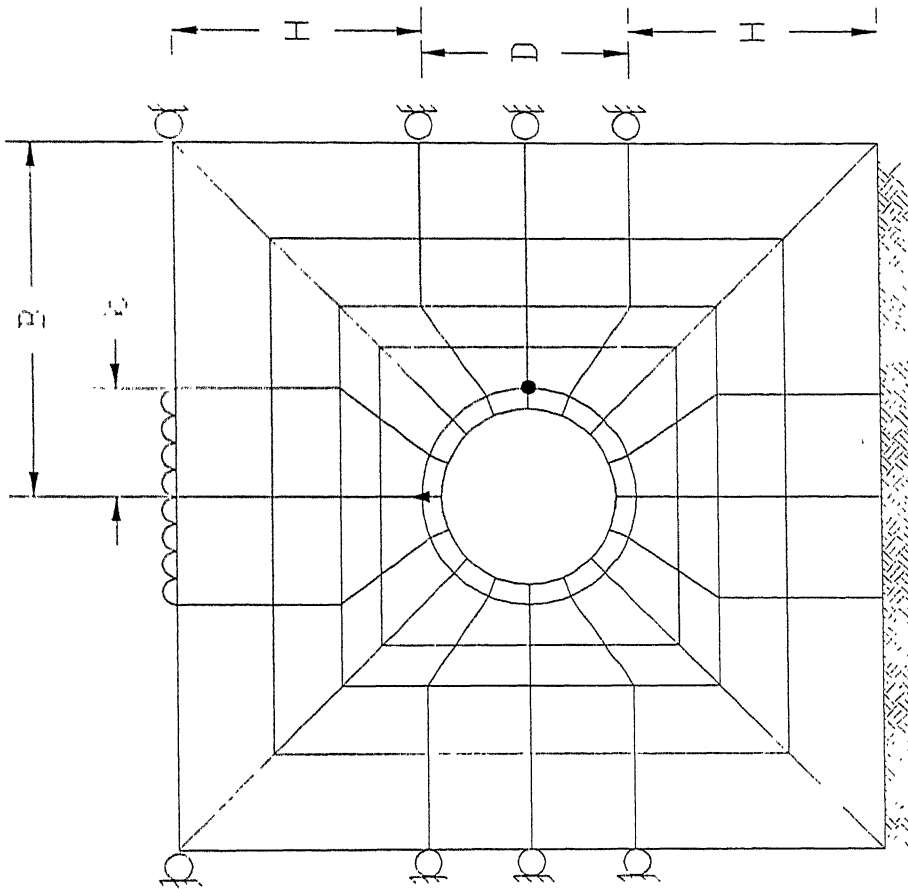
### 3.2.2 Summary

Response of buried circular pipe under static loading has been investigated. The parameters that effect crown and springline response such as load width-to-radius ratio, radius-to-thickness ratio and embedment depth-to-diameter ratio

have been studied. Some of the important observations made from the study are summarized below.

1. Load width-to-radius ratio has significant effect on both the crown and springline response up to a value of 4. Beyond that the crown response remains constant, whereas springline response decreases. The maximum crown response is about 3.5 times that of the maximum springline response.
2. The thickness of pipe does not significantly effect the crown response.
3. Embedment depth has significant effect on both the crown and springline responses. With increase of depth of embedment, the response decreases. The maximum crown response for  $H/D = 1$  is about 1.3 times that of the maximum crown response of  $H/D = 2$ . In case of springline response, the maximum horizontal springline deflection for  $H/D = 1$  is about 1.2 times that of maximum horizontal springline deflection of  $H/D = 2$ .

The results obtained with the present model are compared with those reported by Ramakrishnan (1979) and are shown in Figures 3.3 to 3.7. The results obtained compare well with those reported by Ramakrishnan (1979).



▲ Crown  
● Springline

Fig. 3.1 Problem definition for 3-D pipe-soil system under static loading

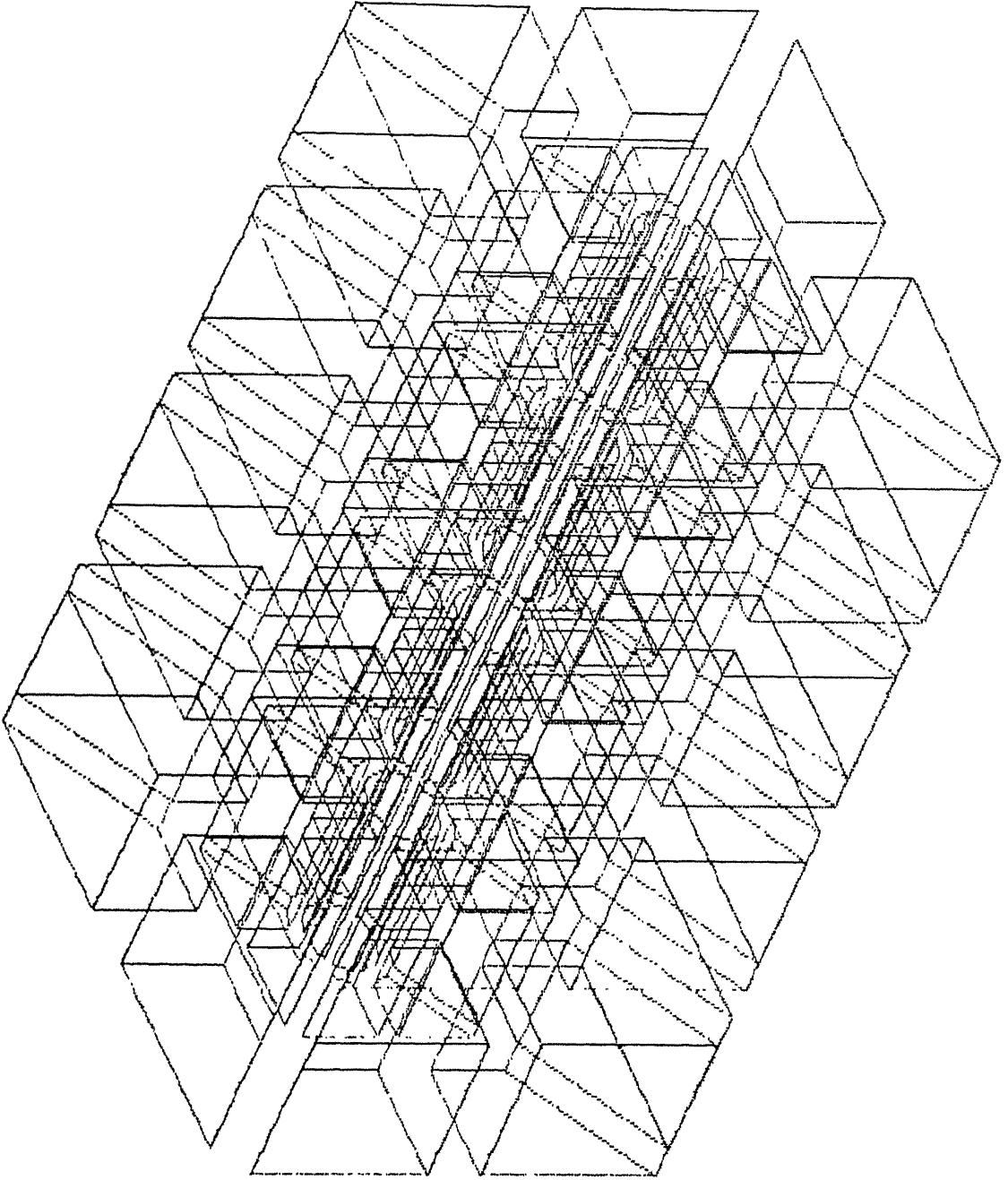


Fig. 3.2 Finite Element Discretization for 3-D Pipe-soil system under static



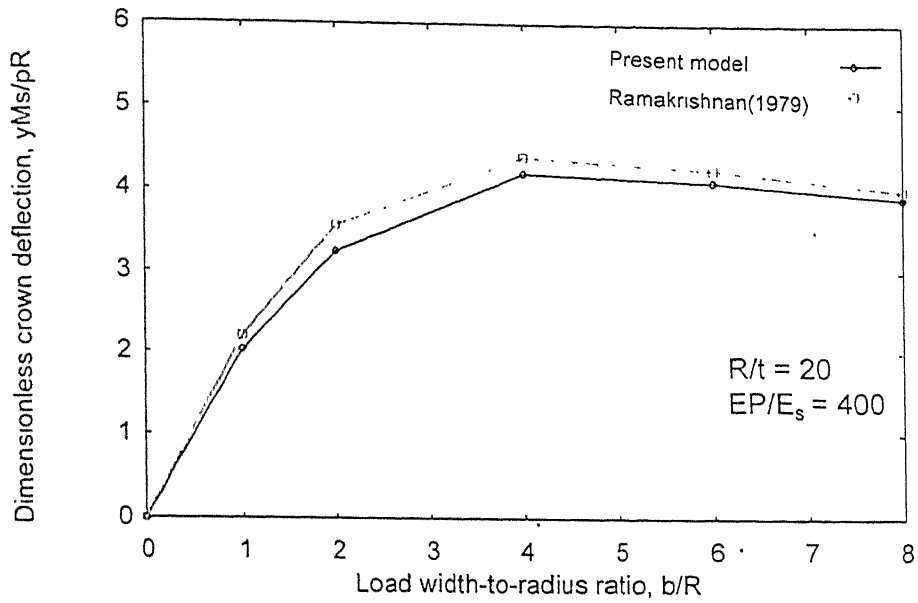


Fig. 3.3 Dimensionless Crown deflection vs Load width-to-radius ratio for  $H/D = 1$

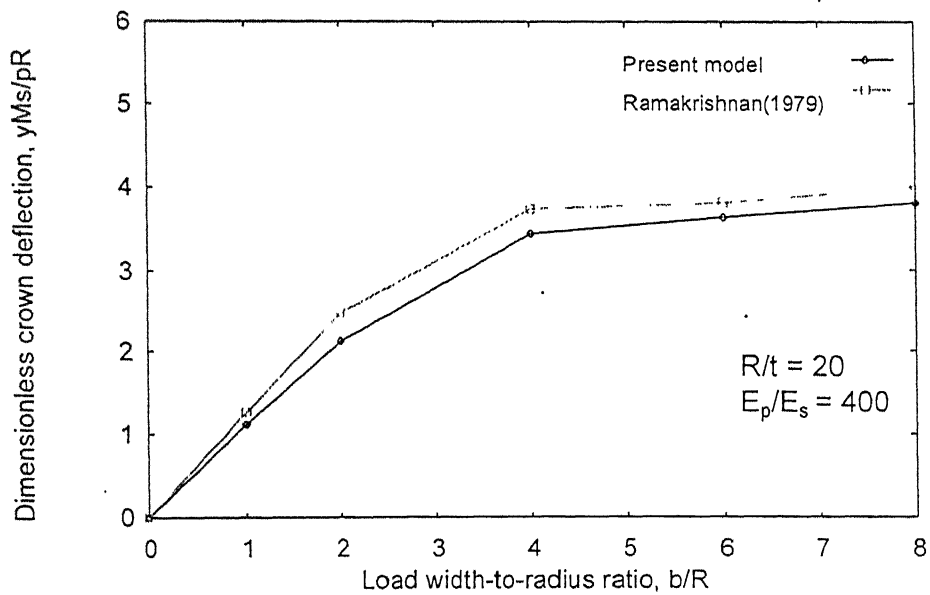


Fig. 3.4 Dimensionless Crown deflection vs Load width-to-radius ratio for  $H/D = 2$

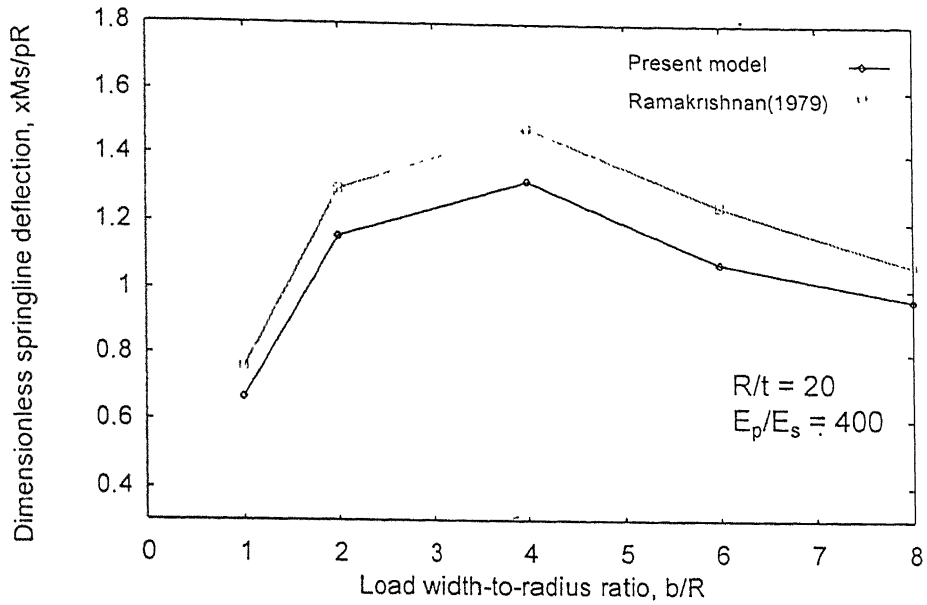


Fig. 3.5 Dimensionless Springline deflection vs Load width-to-radius ratio for  $H/D=1$ .

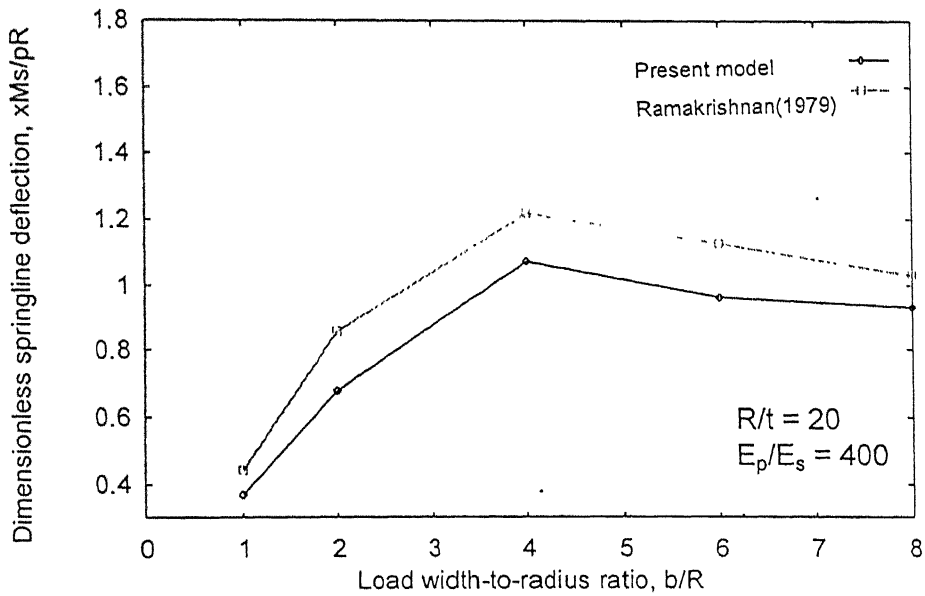


Fig. 3.6 Dimensionless Springline deflection vs Load width-to-radius ratio for  $H/D=2$ .

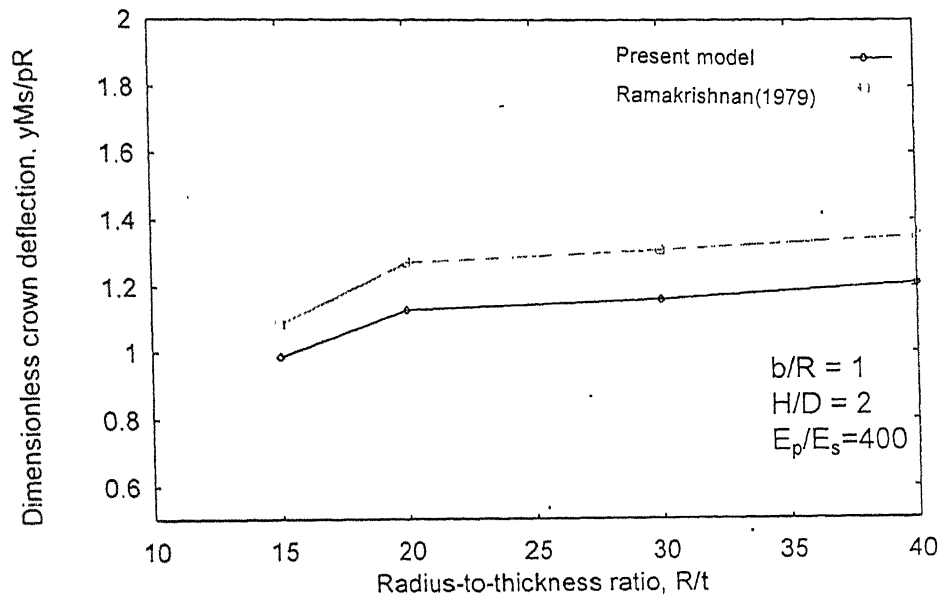


Fig. 3.7 Dimensionless Crown deflection vs Radius-to-thickness ratio.

### 3.3 Problem 2: Response of buried pipe under seismic loading.

#### 3.3.1 Validation of the model

The response of buried pipe-soil system subjected to one dimensional seismic loading (in z-direction) is analysed with the present 3D model. Problem definition and the discretized domain are shown in Figures 3.8 and 3.9. L and D are length, and diameter of pipe respectively; H and t are the depth of embedment and thickness of pipe. The geometry and material properties of the problem analyzed are as follows-

Size of the model : 48 X 10 X 40 m

Number of elements: 384

Young's Modulus of the soil medium  $E_s = 8 \times 10^4$  kPa

Poisson's ratio of the soil medium  $\nu_s = 0.35$

Young's Modulus of the pipe  $E_p = 2.0 \times 10^7$  kPa

Poisson's ratio of the pipe  $\nu_p = 0.2$

Length of the pipe L = 10 m

Diameter of the pipe D = 0.96 m

Depth of embedment H = 7.5 m

##### 3.3.1.1 Input data

El Centro earthquake (California 1940) data is used as the input and is given at the bottom of the model to check the validity of the model. The earthquake data and the response spectra of the El Centro earthquake are shown in the Fig. 3.10 and Fig. 3.11 respectively.

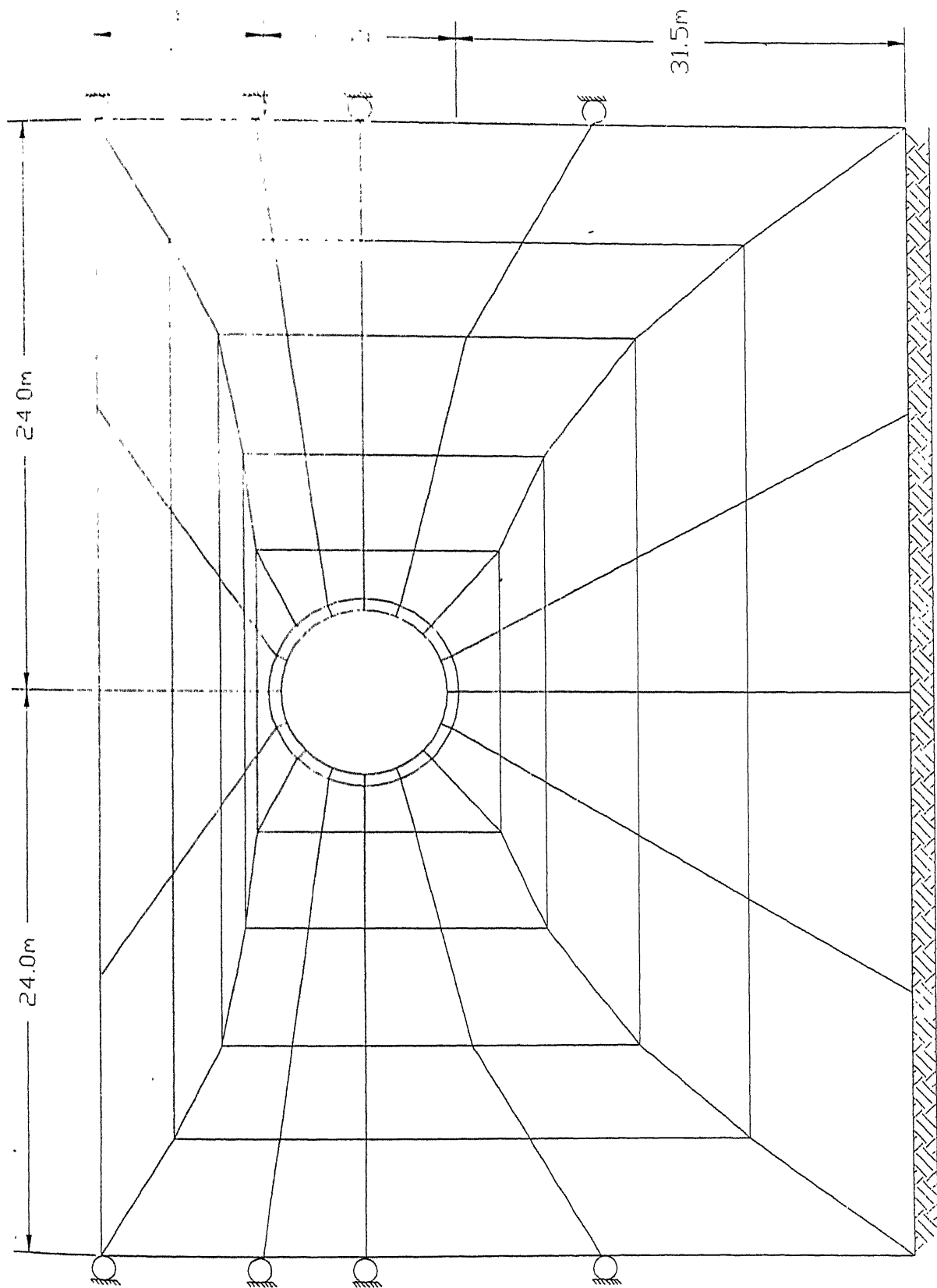


Fig. 3.8 Problem definition for 3-D pipe-soil system under seismic loading

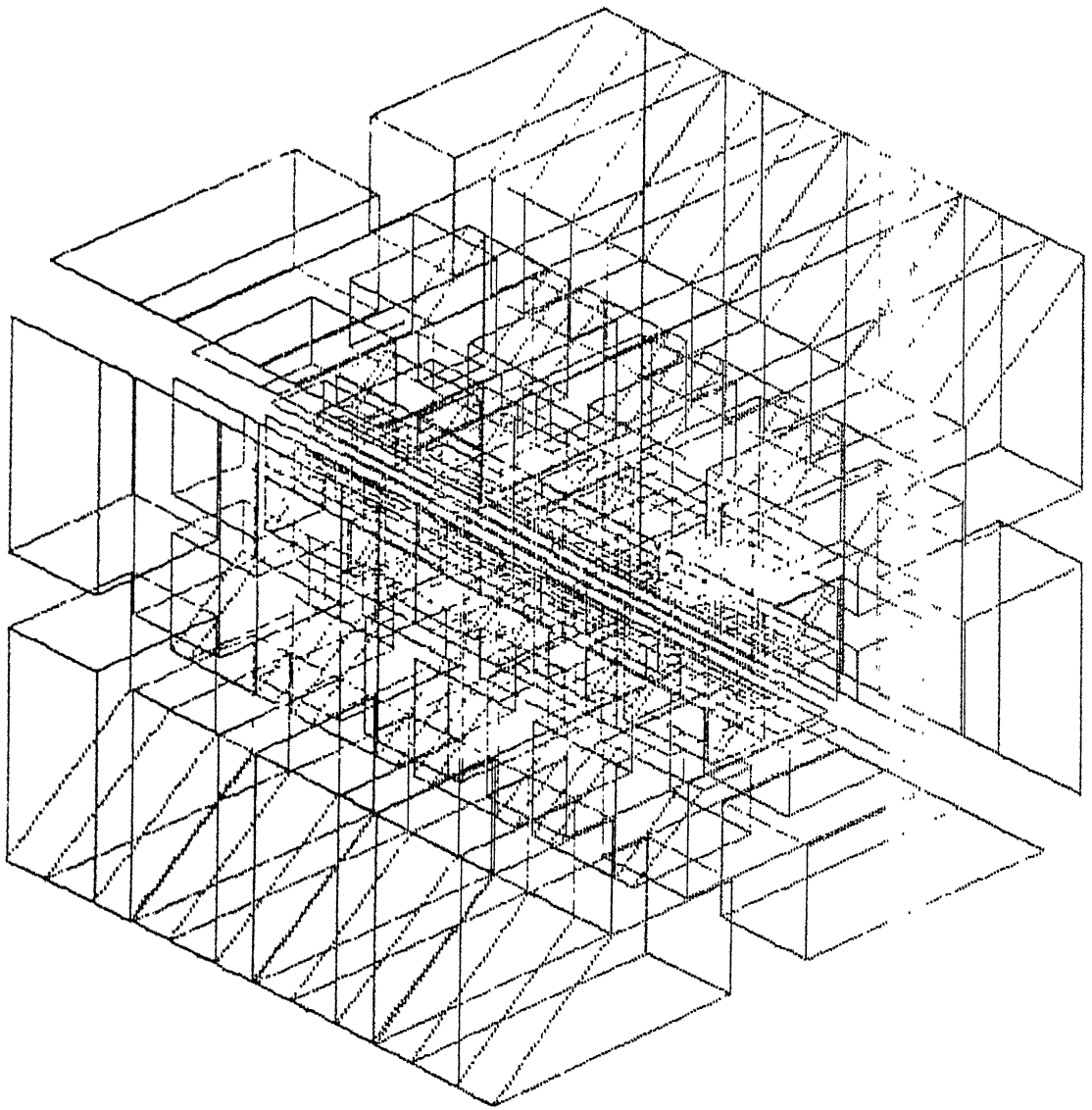


Fig.3.9 Finite Element Discretization for 3D Pipe-soil system under Seismic loading

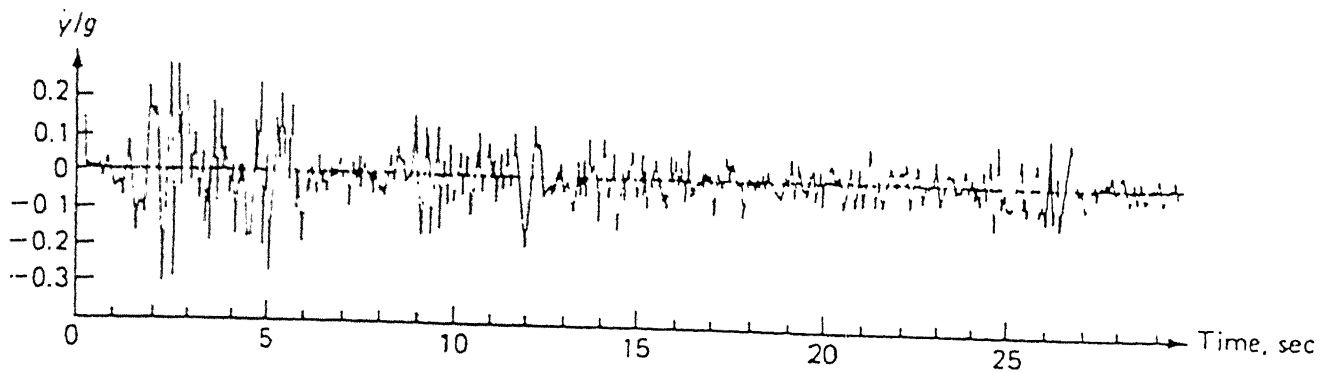


Fig. 3.10 1940 El Centro, California earthquake data

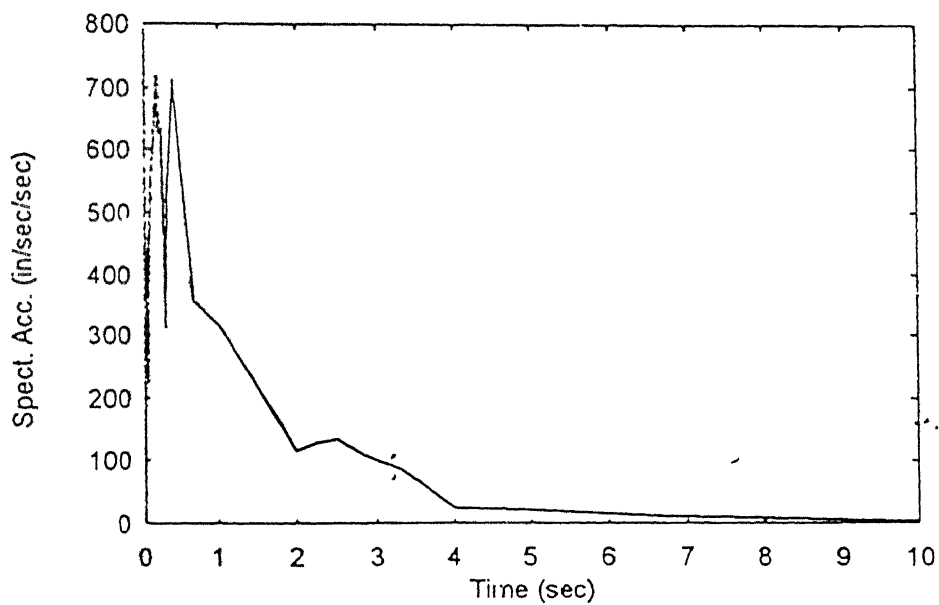


Fig. 3.11 Response spectrum of 1940 El Centro earthquake

### 3.3.1.2 Effect of mode shape number

The effect of mode shape number on the response of crown has been studied, and are shown in Fig. 3.12. The vertical crown deflection increases with increasing the mode shape number up to a value of 10 and beyond that the response remains constant.

The results obtained are tabulated in Table 3.1 and are compared with the results reported by Haldar, A. K. et. al. (1980).

Table 3.1 Responses under different earthquakes

Name of earthquake	Intensity of earthquake	Vert. Crown response
Modified 1940 EI Centro (present model)	0.165g	25.1 mm
1952 California (Haldar model)	0.153g	20.8 mm

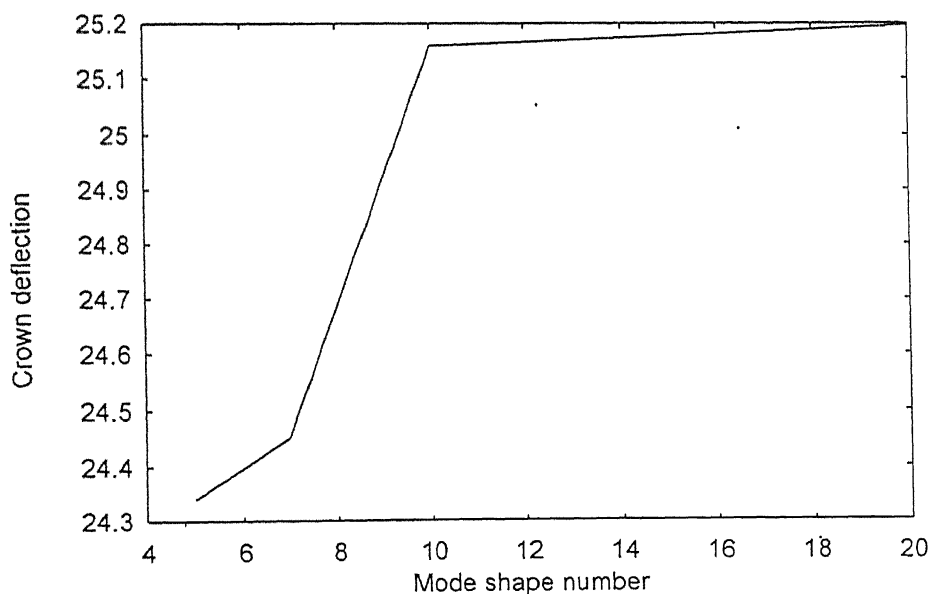


Figure 3.12 Response vs Mode shape number



### 3.3.2 Parametric studies

The effect of various parameters on the responses like vertical crown displacement and horizontal springline displacement are studied with present 3D model. The projected discretized model on x-z plane has been shown in Fig. 3.13. The geometry and material properties used are as follows-

Size of the model : 40 X 10 X 11 m

Number of elements: 384

Young's Modulus of the soil medium  $E_s = 1 \times 10^4$  kPa or variable

Poisson's ratio of the soil medium  $\nu_s = 0.3$

Young's Modulus of the pipe  $E_p = 4.0 \times 10^6$  kPa

Poisson's ratio of the pipe  $\nu_p = 0.2$

Length of the pipe  $L = 10$  m

Diameter of the pipe  $D = 1.0$  m

Depth of embedment  $H = 4.0$  m or variable

The seismic data shown in Fig. 3.10 and Fig. 3.11 are used as input and the effect of the following parameters on the responses have been studied.

- a) Effect of three dimensional seismic loading
- b) Effect of mode shape numbers
- c) Effect of radius-to-thickness ratio
- d) Effect of  $E_p/E_s$  ratio
- e) Effect of embedment depth
- f) Effect of liquefied soil zone

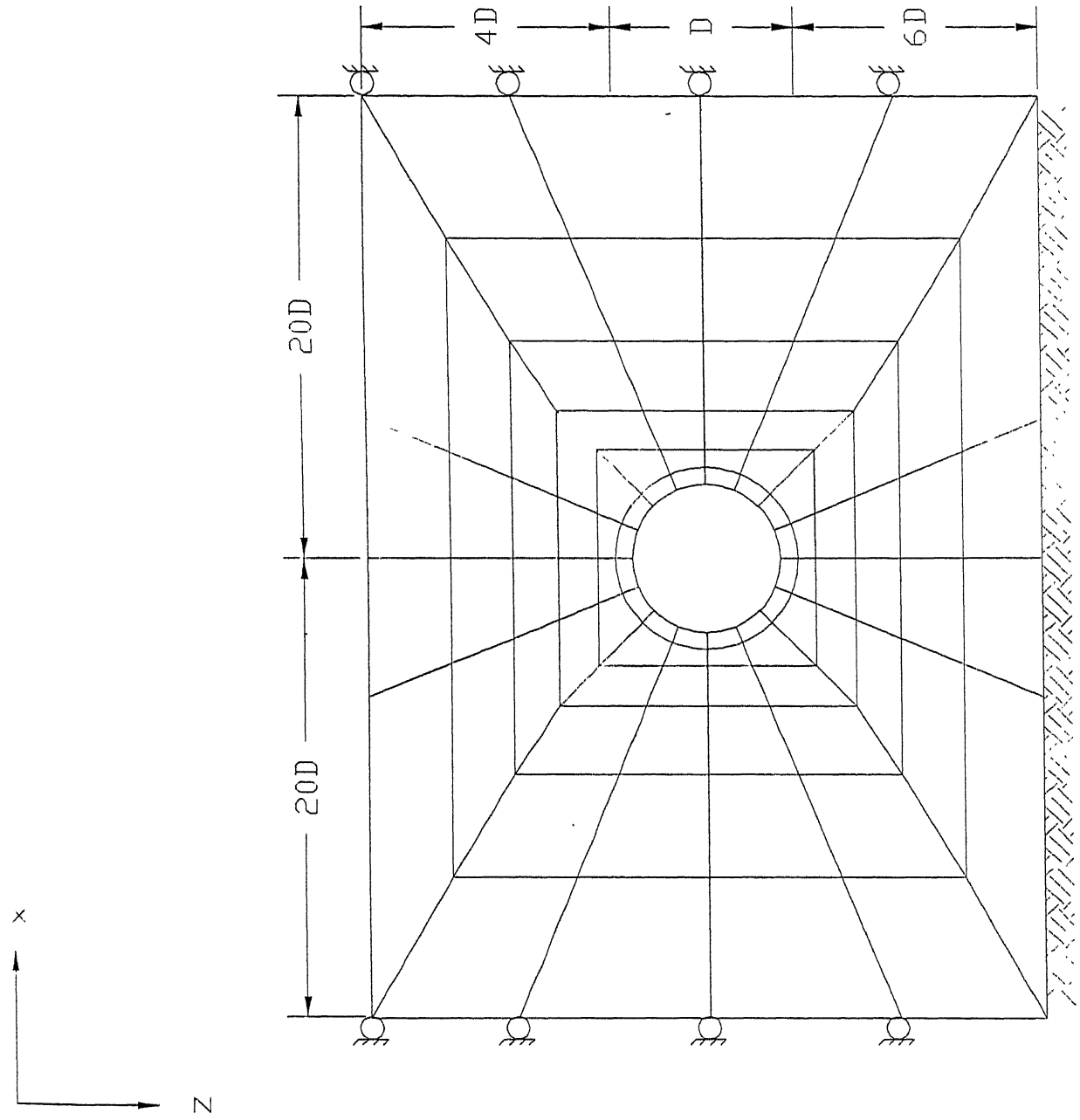


Fig. 3.13 Projected Discretized model on  $x$ - $z$  plane

### 3.3.2.1 Effect of three dimensional seismic loading

The effect of three dimensional loading on the responses are obtained by applying the seismic loading (Fig. 3.10, 3.11) in three mutually perpendicular (x, y, z) directions to the model shown in Fig. 3.13. The vertical crown displacement and the horizontal springline displacement are tabulated in Table 3.2 and are compared with the responses of 1-D (applied in z direction only) seismic loading. The values of  $E_p/E_s = 250$ ,  $R/t = 20$ ,  $H/D = 4$  and  $V = 15$  are taken.

Table 3.2 Effect of 3-D seismic loading on responses

Crown resp. under 1-D loading mm	Crown resp. under 3-D loading mm	Springline resp. under 1-D loading mm	Springline resp. under 3-D loading mm
19.08	38.71	1.82	24.25

### 3.3.2.2 Effect of mode shape number

The responses of pipe for various mode shape numbers have been studied. They are studied for a  $R/t$  ratio of 20,  $E_p/E_s$  of 250, and  $H/D$  ratio of 4.

**Springline displacement:** The springline displacement variation with mode shape number is shown in Fig. 3.14. The horizontal springline displacement remains almost constant with increasing the mode shape number.

**Crown displacement:** The crown displacement variation with mode shape number is shown in Fig. 3.14. The vertical crown displacement increases with mode shape number up to a value 15, beyond that the displacement tends to be constant.

### 3.3.2.3 Effect of $E_p/E_s$ ratio

The responses of pipe for various  $E_p/E_s$  ratios have been studied. They are studied for a  $R/t$  ratio of 20, mode shape number  $V$  of 15, and  $H/D$  ratio of 4.

**Springline displacement:** The horizontal springline displacement variation with  $E_p/E_s$  is shown in Fig. 3.15. With the increase of  $E_p/E_s$  i.e. decrease of strength in soil, increases the horizontal springline displacement.

**Crown displacement:** The vertical crown displacement variation with  $E_p/E_s$  is shown in Fig. 3.15. similar trend of springline displacement has been observed in vertical crown displacement case.

### 3.3.2.4 Effect of radius-to-thickness ratio

The responses of pipe for various  $R/t$  ratios have been studied. They are studied for a  $E_p/E_s$  ratio of 250, mode shape number  $V$  of 15, and  $H/D$  ratio of 4.

**Springline displacement:** The horizontal springline displacement variation with  $R/t$  is shown in Fig. 3.16. With the increase of  $R/t$  i.e. decrease of thickness of pipe, increases the horizontal springline displacement, but the large increase in the thickness changes the springline displacement only a small amount.

**Crown displacement:** The vertical crown displacement variation with  $R/t$  is shown in Fig. 3.16. similar trend of springline displacement has been observed in vertical crown displacement case.

### 3.3.2.5 Effect of embedment depth

The responses of pipe for various  $H/D$  ratios have been studied. They are studied for a  $E_p/E_s$  ratio of 250,  $V$  of 15, and  $R/t$  ratio of 20.

**Springline displacement:** The springline displacement variation with  $H/D$  is shown in Fig. 3.17. The horizontal springline displacement remains almost constant with increasing the  $H/D$  ratio.

**Crown displacement:** The crown displacement variation with  $H/D$  is shown in Fig. 3.17. The vertical crown displacement remains constant with  $H/D$  ratio up to a value 2, beyond that the crown displacement tends to be increasing.

### 3.3.2.6 Effect of liquefied soil zone

Liquefaction is a state of soil when it becomes unstable. When effective stress in soil reduces to zero, the soil loses its shear strength then it behaves like a slurry and flows like a liquid. Liquefaction is usually associated with the earthquakes. The effect of cyclic process of liquefaction of soil on responses has been studied by considering a soil zone of 1.5 times the diameter of the pipe around the buried pipe. The Young's Modulus of this soil  $E_{ls}$ , taken as  $1/10$ , and  $1/20$  of the original soil modulus value. The responses under these conditions are tabulate in Table 3.3. the values of  $E_p/E_s = 250$ ,  $R/t = 20$ ,  $V = 15$  and  $H/D = 4$  are taken in this study.

Table 3.3 Effect of liquefied soil zone on responses

Response	With liquefaction zone		with out liquefaction zone
	$E_{ls} = E_s/10$	$E_{ls} = E_s/20$	
Springline displacement mm	26.17	28.19	24.25
Crown displacement mm	42.63	44.68	38.71

### 3.3.3 Summary

Response of buried pipe under seismic loading has been investigated. The effect of 3-D seismic loading, mode shape number,  $R/t$  ratio,  $E_p/E_s$  ratio, embedment depth and liquefied soil zone have been studied. A summary of the observations made from the parametric study conducted are presented below.

1. Three dimensional seismic loading has stronger influence on responses than the one dimensional seismic loading. The maximum crown response under 3-D loading is almost double that of the maximum crown response under 1-D loading. In case of springline response, the maximum horizontal springline deflection under 3-D loading is about 14 times the maximum horizontal springline deflection under 1-D loading (Ref. Tab. 3.2)
2. The mode shape number has very little effect on springline response, whereas in case of crown response it has significant effect up to a value of 15.
3. With decreasing soil strength i.e., with increasing modular ratio, the pipe responses are increasing. The modular ratio has greater effect on crown response than that of springline response.
4. The pipe thickness does not significantly effect the vertical crown and horizontal springline response.
5. The embedment depth has little effect on horizontal springline response, but in case of crown response it has significant effect beyond  $H/D = 2$ .
6. Liquefaction zone in soil surrounding the buried pipe has significant effect on pipe responses.

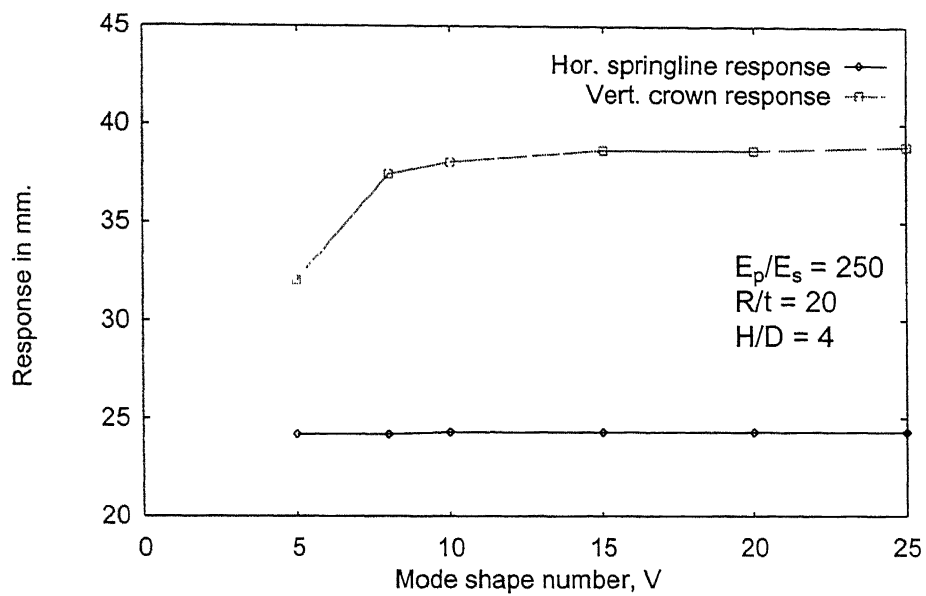


Fig. 3.14 Response vs Mode shape number

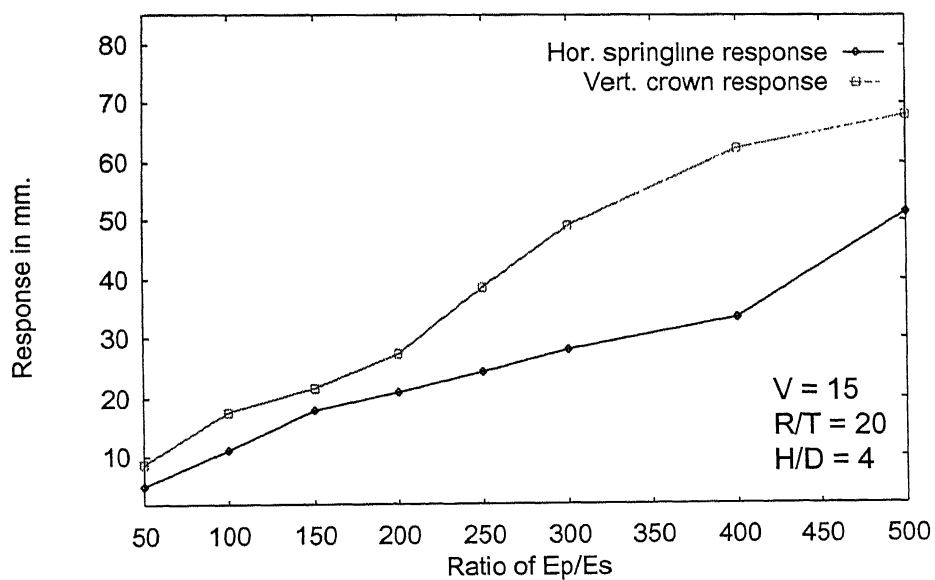


Fig. 3.15 Response vs  $E_p/E_s$  ratio

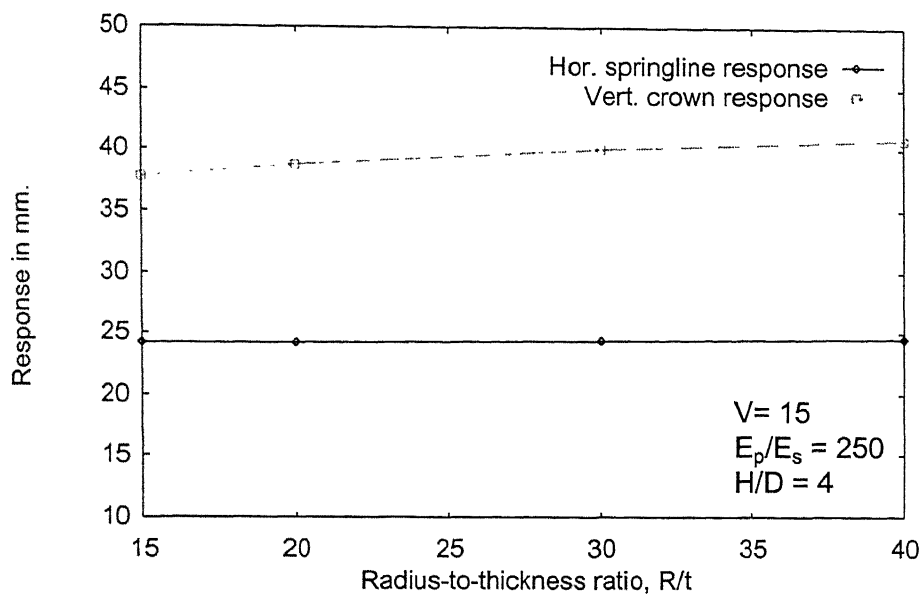


Fig. 3.16 Response vs Radius-to-thickness ratio

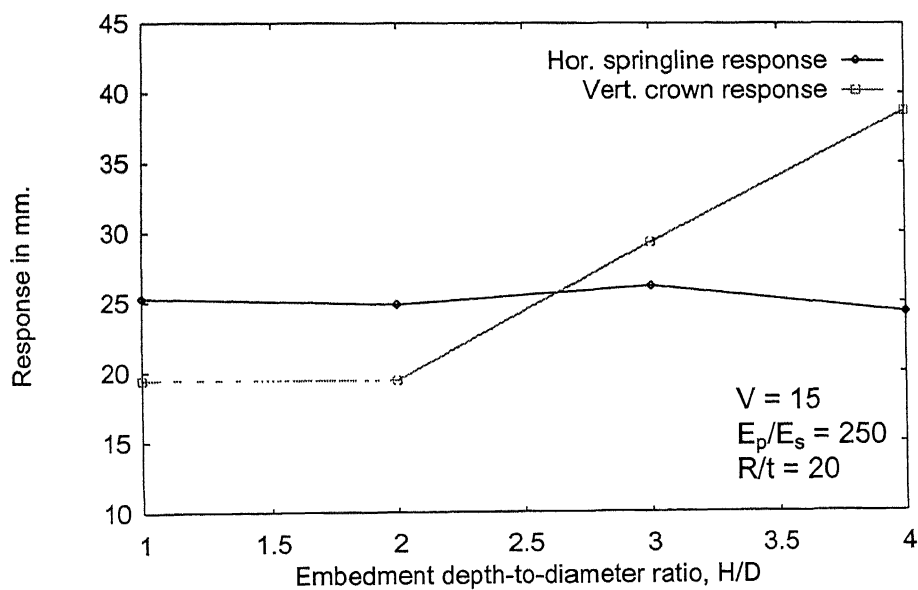


Fig. 3.17 Response vs Embedment depth-to-diameter ratio



## **Chapter 4**

### **Conclusions and Scope for future study**

#### **4.1 General**

The results obtained in the present study for different class of problems have already been discussed in the previous Chapter. The conclusions, possible extensions of the study and scope are presented in the following sections.

#### **4.2 Conclusions**

In this investigation the response of buried pipe under different load conditions has been studied using finite element method package SAP-80. Pipe-soil system is discretized using 3-D solid elements. Effect of different parameters on pipe response are studied using mode super position method.

From the results obtained for different problems solved in Chapter 3, it can be seen that the present 3-D model was more effective in determining the response of pipe under general earthquake loading.

#### **4.3 Scope for future study**

Few possible extensions of the present study could be in the following directions.

1. Incorporation of non-linear and non-homogeneous material models.
2. Incorporation of interface (contact) elements to account for slippage of pipe-soil system.
3. Effect of shape of pipe and elevation difference of pipe ends.
4. More detailed study of liquefaction effect on pipe response.

## References

- Abel, J. F. , Mark, R. and Richards, R. (1973).** "Stresses around flexible elliptic pipes". *Journal of the Soil Mechanics and Foundations Division, ASCE.* , vol. 99, pp. 509-526.
- Akiyoshi, T. and Fuchida, K. (1982).** "Soil-pipeline interaction through a frictional interface during earthquakes". *Soil Dynamics and Earthquake Engineering Conference*, pp. 497-511.
- Anand, S. C. (1974).** "Stress distribution around shallow buried rigid pipes". *Journal of Structural Division, ASCE.* , vol. 100, pp. 161-174.
- Ariman, T. and Muleski, G. E. (1981).** "A review of the response of buried pipelines under seismic excitations". *Earthquake Engineering and Structural Dynamics*, vol. 9, pp. 133-151.
- Brown, C. B. (1967).** "Forces on rigid culverts under high fills". *Journal of Structural Division, ASCE.* , vol. 93, pp. 195-215.
- Brown, C. B. , Green, D. R. and Pawsey (1968).** "Flexible culverts under high fills". *Journal of Structural Division, ASCE.* , vol. 94, pp. 905-917.
- Datta, S. K. , Shah, A. H. and Wong, K. C. (1984).** "Dynamic stresses and displacements in buried pipe". *Journal of Engineering Mechanics Division ASCE.*, vol. 110, pp. 1451-1466.
- Datta, S. K. , Shah, A. H. , O'Leary, P. M. and Wong, K. C. (1984).** "Seismic reponse analysis of embedded pipelines". *Journal of Engineering Mechanics Division ASCE.* , pp. 23-32.
- Datta, T. K. and Mashaly, E. A. (1986).** "Pipeline response to random ground motion by discrete model". *Earthquake Engineering and Structural Dynamics*, vol. 14, pp. 559-572.
- Datta, T. K. and Mashaly, E. A. (1990).** "Transverse response of offshore pipelines to random ground motion". *Earthquake Engineering and Structural Dynamics*, vol. 19, pp. 217-228.
- Desai, C. S. and Abel, J. F. (1972).** "Introduction to finite element method". *Affiliated East-West press (pvt.) Ltd. , New Delhi.*
- Haldar, A. K. , Reddy, D. V. , Arockiasamy, M. and Bobby, W. (1980).** "Finite element nonlinear seismic response analysis of submarine pipe-soil

interaction". *International symposium on soils under cyclic and transient loading, Swansea.*

**Hindy, A. and Novak, M. (1980).** "Pipeline response to random ground motion". *Journal of Engineering Mechanics Division ASCE.* , vol. 106, pp. 339-360.

**Hindy, A. and Novak, M. (1980).** "Earthquake response of buried insulated pipes". *Journal of Engineering Mechanics Division ASCE.* , vol. 106, pp. 1135-1149.

**Hoeg, K. (1968).** "Stresses against underground structural cylinders". *Journal of the Soil Mechanics and Foundations Division, ASCE.* , vol. 94, pp. 844-858.

**Mariopaz (1985).** "Microcomputer-aided Engineering Structural Dynamics". *Von Nostund Reinhold Co.* , Newyork.

**Nabil, E. A. and Datta, S. K. (1981).** "Response of a circular cylindrical shell to disturbances in a halfspace - numerical results". *Earthquake Engineering and Structural Dynamics*, vol. 9, pp. 477-487.

**Prakash, S. , Nayak, G. C. and Gupta, R. (1976).** "Analysis of buried pipes under embankment". *Numerical Methods in Geomechanics ASCE.* , vol. 2, pp. 886-900.

**Ramakrishnan, K. (1979).** "Finite element analysis of pipes buried in linear and nonlinear elastic media". *M.Tech. Thesis, I. I. T. Kanpur.*

**Sakib, H. and Abdolsalami, N. (1995).** "Analysis of buried pipelines to random ground motions in homogeneous medium". *10th European conference on Earthquake Engineering, Duma.*

**Stamos, A. A. and Beskos, D. E. (1995).** "Dynamic analysis of large 3-D underground structures by the boundary element method". *Earthquake Engineering and Structural Dynamics*, vol. 24, pp. 917-934.

**Valliappan, S. , Matsuzaki, K. and Rajasekar, H. L. (1977).** "Nonlinear stress analysis of buried pipes". *Proceedings, International symposium on soil-structure interaction, Univesity of Roorkee.*

**Venugopal Rao, R. (1995).** "Time domain analysis of three dimensional soil-structure interaction problems". *Ph. D Thesis, I. I. T. kanpur.*

**Wilson, E.I , Der Kiureghian, A. and Bayo, E. P. (1981).** "A replacement for the square-root-sum-of-squares (srss) method in seismic analysis". *Earthquake Engineering and Structural Dynamics*, vol. 9, pp. 187-194.

**Wilson, E. L. and Habibullah, A. (1984).** "SAP80 manual", *Structural analysis programs, Berkely, California.*

**Yeh, Y. and Wang, L. R. (1985).** "Dynamic response of buried pipelines in a soil liquefaction environment during earthquakes". *5th International conference on numerical methods in Geomechanics, Nagoya.*

**Zerva, A. , Ang, A. H. S. and Wen, Y. K. (1988).** "Lifeline response to spatially variable ground motions". *Earthquake Engineering and Structural Dynamics*, vol. 16, pp. 361-379.